POLITECNICO DI TORINO

Collegio di Ingegneria Chimica e dei Materiali

Master of Science Course
in Materials Engineering

Master of Science Thesis

Micromagnetic Simulation of Ferromagnetic Nanowires

Tutors
Marco César Maicas Ramos
Josè Luis Prieto Martin
Fausto Rossi

Candidate
Adele Valpreda

October 2020

Micromagnetic Simulation of Ferromagnetic Nanowires

Master thesis project developed within the

ERASMUS PROGRAM E+/EU PROGRAMME COUNTRIES

at

Universidad Politécnica de Madrid

Escuela Técnica Superior de Ingenieros de Caminos, Canales y Puertos

Academic year

2019/2020

Riassunto

Nei campi dell'ingegneria, e delle discipline scientifiche in generale, simulazioni numeriche sono spesso utilizzate per completare studi teorici e sperimentali. Nell'ambito della ricerca e sviluppo di dispositivi magnetici, le simulazioni denominate Computational Micromagnetic Simulations sono uno strumento di fondamentale importanza perché permettono non solo di simulare e predire la risposta magnetica a livello macroscopico (ciclo d'isteresi o Hysteresis loop) di un campione, ma anche di osservare la distribuzione dei momenti magnetici (Magnetic texture) che è una caratteristica difficile da osservare tramite studi sperimentali [1,2,3].

Per il presente studio si è fatto uso del programma OOMMF, acronimo di Object Oriented MicroMagnetic Framework, un programma open source scritto in C++ [4].

L'input del programma è un file di testo, chiamato Configuration file. Tale file di testo, che viene scritto nel linguaggio Tcl, è il mezzo per stabilire la geometria del campione, i materiali che lo costituiscono e per definire i parametri di simulazione. Il primo obbiettivo di questo progetto è stata la scrittura di tale Configuration file per simulare la risposta magnetica di un nanowire ferromagnetico.

Nel caso di strutture nanometriche, come in questo caso, l'interazione con il materiale circostante è di particolare interesse; per questo motivo, il Configuration file che è stato sviluppato permette di modellizzare non solo un semplice nanowire di un determinato materiale ferromagnetico ma anche una struttura cilindrica Core-Shell. Variando alcuni parametri che definiscono l'interfaccia, è stato possibile studiare l'interazione tra il materiale ferromagnetico del nanowire ed il materiale circostante.

Il secondo obiettivo del lavoro di tesi è stato lo studio di come la risposta magnetica (Hysteresis loop e Magnetic texture) di un nanowire ferromagnetico sia influenzata dalla geometria e dal tipo di materiale ferromagnetico.

I nanowire sono nanostrutture 1D, caratterizzate dunque da un elevato rapporto di forma (aspect ratio). Tale caratteristica fa si che i nanowire ferromagnetici presentino risposte magnetiche uniche, e ciò li rende ottimi candidati per diverse applicazioni, ad esempio in nanoelettronica come Recording Media per memorie magnetiche [2,3,5].

Per via della sua geometria, all'equilibrio, la Magnetic texture di un nanowire ferromagnetico è tipicamente con i momenti magnetici allineati con l'asse del nanowire. Quando sottoposto ad un forte campo magnetico esterno nella direzione opposta, il nanowire inverte la direzione dei momenti magnetici. Tale processo, chiamato Magnetization Reversal Process tipicamente avviene attraverso la nucleazione e propagazione di un Domain wall (parete di dominio magnetico). A parità di geometria, il tipo di Domain wall, e dunque il tipo di reversal process, dipende dal materiale e del mezzo circostante. Per la realizzazione di memorie magnetiche, e per altre potenziali applicazioni di nanowire ferromagnetici, il controllo del Magnetization Reversal Process è fondamentale [5].

Per questo studio, si sono utilizzati due materiali ferromagnetici, nichel e cobalto. Per tutte le simulazioni si sono utilizzati nanowire di lunghezza 1 µm e di diametro nel range 40 nm-80 nm.

Per prima cosa, la simulazione della risposta magnetica di tre nanowire di nichel ha permesso di analizzare come la forma (ed in particolare l'aspect ratio) influenzi il Magnetization Reversal Process. Si sono condotte tre simulazioni su nanowire di lunghezza 1 µm e di diametro variabile (40 nm, 60 nm e 80 nm). Confrontando i risultati è stato possibile osservare che, a seconda del diametro, il Magnetization Reversal Process può avvenire attraverso la formazione di un domain wall cosiddetto Trasversale oppure con un domain wall a Vortice.

Successivamente, tre nanowire di cobalto sono stati modellati per osservare come la struttura cristallina causi anisotropia nella risposta magnetica. In un nanowire ferromagnetico la direzione definita easy-axis rappresenta la direzione verso cui i momenti magnetici tendono per via del reticolo cristallino. A parità di geometria e di campo

magnetico esterno applicato, se l'asse verso cui tende la magnetizzazione (easy-axis) è differente, la risposta magnetica del materiale è differente. Per studiare tale fenomeno, durante le tre simulazioni si è cambiato l'angolo di deviazione β tra l'easy-axis e il campo magnetico applicato. È stato possibile osservare che nel caso di nanowire di cobalto la risposta magnetica dipende fortemente dall'angolo di deviazione.

Per studiare l'interazione con il materiale circostante, una struttura Core-Shell di cobalto (Co) e ossido di cobalto (CoO) è stata modellata. Tale sistema ha permesso di analizzare un fenomeno chiamato Exchange Bias effect. All'interfaccia tra i due materiali vi è un accoppiamento dei momenti magnetici. La principale conseguenza a livello macroscopico e uno shift del ciclo d'isteresi (Hysteresis loop). Con il modello sviluppato (Configuration file) è stato possibile simulare l'effetto di accoppiamento all'interfaccia (Exchange Bias effect) in quanto nella risposta magnetica si osserva uno shift del ciclo d'isteresi.

Si sono condotte tre simulazioni con un diverso valore di costante di accoppiamento all'interfaccia. Tali simulazioni hanno per messo di verificare che lo shift è controllato dall'intensità dell'accoppiamento tra i momenti magnetici dell'interfaccia. È stato inoltre possibile verificare che l'Exchange Bias è un effetto superficiale, la cui efficacia dipende dal rapporto interfaccia/volume.

Resumen

En el ámbito de la ingeniería, las simulaciones numéricas se utilizan frecuentemente para completar estudios teóricos y experimentales. En el campo de la investigación y desarrollo de dispositivos magnéticos, las simulaciones conocidas como Computational Micromagnetic Simulations son un instrumento de gran importancia porque permiten no solo simular la respuesta magnética a nivel macroscópico (bucle de histéresis o hysteresis loop) de una muestra, sino que también permiten observar la distribución de momentos magnéticos (magnetic texture) que es una característica difícil de observar a través de estudios experimentales [1,2,3].

Para el presente estudio se ha utilizado el programa OOMMF, acrónimo de Object Oriented MicroMagnetic Framework, un programa de código escrito en C++ [4].

El input del programa es un archivo de texto, llamado Configuration file. Este archivo de texto, que está escrito en lenguaje Tcl, es el medio para establecer la geometría de la muestra, los materiales que la constituyen y para definir los parámetros de simulación. El primer objetivo de este proyecto ha sido la escritura de este Configuration file para simular la respuesta magnética de un nanowire ferromagnético.

En el caso de estructuras nanométricas, como en este caso, la interacción con el material circundante tiene una importancia fundamental; por esta razón, el Configuration file escrito para este trabajo permite modelar no solo un simple nanowire de un material ferromagnético específico, sino también una estructura cilíndrica Core-Shell. Variando algunos parámetros que definen la interfaz, fue posible estudiar la interacción entre el material ferromagnético del nanowire y el material circundante.

El segundo objetivo de esta tesis fue el estudio de la influencia de la geometría y el tipo de material ferromagnético en la respuesta magnética (bucle de histéresis y magnetic texture) de un nanowire ferromagnético.

Los nanowires son nanoestructuras 1D, por lo que se caracterizan por una alta relación de aspecto (aspect ratio). Esta característica lleva a respuestas magnéticas únicas, y por esto los nanowires ferromagnéticos son excelentes candidatos para diferentes aplicaciones. Por ejemplo, en nanoelectrónica como medios de grabación para memorias magnéticas [2,3,5].

Debido a su geometría, en equilibrio, la magnetic texture de un nanowire ferromagnético se encuentra típicamente con los momentos magnéticos alineados con el eje del nanowire. Cuando se somete a un fuerte campo magnético externo en la dirección opuesta, el nanowire invierte la dirección de los momentos magnéticos. Este proceso, llamado Magnetization Reversal Process, típicamente ocurre a través de la nucleación y propagación de un domain wall (pared de dominio magnético). El tipo de domain wall depende del material y del medio circundante. Para la realización de memorias magnéticas, y para otras potenciales aplicaciones de los nanowires ferromagnéticos, el control de este Magnetization Reversal Process es fundamental [5].

Para este estudio se utilizaron dos materiales ferromagnéticos, níquel y cobalto. Para todas las simulaciones se utilizaron nanowires con una longitud de 1 µm y un diámetro en el rango de 40 nm a 80 nm.

Primero, la simulación de la respuesta magnética de tres nanowires de níquel nos permitió analizar cómo la forma (y en particular la relación de aspecto) afecta el proceso de inversión de magnetización. Se realizaron tres simulaciones en nanowires de 1 µm de longitud y diámetro variable (40 nm, 60 nm y 80 nm). Al comparar los resultados se pudo observar que, dependiendo del diámetro, el Proceso de Reversión de la Magnetización puede tener lugar a través de la formación de un domain wall llamado Transversal o con un domain wall llamado Vortex.

Posteriormente, se modelaron tres nanowires de cobalto para observar cómo la estructura cristalina provoca anisotropía en la respuesta magnética. En un nanowire ferromagnético, la dirección definida como easy-axis representa la dirección hacia la que tienden los momentos magnéticos debido a la red cristalina. Con la misma geometría y campo magnético externo aplicado, si el eje hacia el que tiende la magnetización (easy-axis) es

diferente, la respuesta magnética del material es diferente. Para estudiar este fenómeno, se modificó el ángulo de desviación β entre el easy-axis y el campo magnético aplicado. Se ha podido observar que en el caso de nanowires de cobalto la respuesta magnética depende fuertemente del ángulo de desviación.

Para estudiar la interacción con el material circundante, se modeló una estructura Core-Shell de cobalto (Co) y oxido de cobalto (CoO). Este sistema permitió analizar un fenómeno denominado Exchange Bias effect. En la interfaz entre los dos materiales hay un acoplamiento de los momentos magnéticos. La principal consecuencia a nivel macroscópico es un cambio en el ciclo de histéresis (Hysteresis loop). Con el modelo desarrollado en este estudio (Configuration file) fue posible simular el efecto de acoplamiento a la interfaz (Exchange Bias effect) porque ha sido posible observar un cambio en el ciclo de histéresis (Hysteresis loop).

Se realizaron tres simulaciones con tres valores diferente de acoplamiento en la interfaz. Estas simulaciones han permitido verificar que el desplazamiento está controlado por la intensidad del acoplamiento entre los momentos magnéticos de la interfaz. También se pudo comprobar que el Exchange Bias es un efecto de superficie, cuya efectividad depende de la relación interfaz / volumen.

Summary

Computational simulations are widely used across the engineering and science disciplines to complete experimental and theoretical studies. In the research and development of magnetic devices, computational micromagnetic simulations are a powerful tool that allows not only to predict the macroscopic magnetic response of a sample (Hysteresis Loop), but also to understand the microscopic distribution of magnetic moments (the Magnetic Texture) that is otherwise difficult to explore with experimental tests $[1, 2, 3]$.

The present work makes use of the micromagnetic simulation program OOMMF (Object Oriented MicroMagnetic Framework), which is an open source program written in C++ $[4]$. The input for the program is a configuration file: a text file written in the Tcl syntax that is used to define the sample geometry, the materials that characterize the sample, and the simulation conditions (for example the applied external magnetic field).

The first aim of this study was to write the **Configuration file** (Model) to simulate the magnetic response of a nanowire. The interaction with the surrounding media is of particular interest; for this reason the developed file allows to model not only a cylindrical nanowire of a specified ferromagnetic material, but also a Core-Shell structure of two different materials and define the interaction at the interface.

The second purpose of this thesis-project was to study how the magnetic response (Hysteresis loop and Magnetic texture) of a ferromagnetic nanowire is influenced by wire geometry, by materials parameters and by the interaction with the surrounding material.

Nanowires are 1D nanostructure that exhibit an enhanced aspect ratio. This high value of shape anisotropy leads to unique magnetic properties and makes nanowires promising candidates for applications in nanoelectronics, for example as recording media in magnetic memories $[2, 3, 5]$.

Due to its elongated shape, the magnetic texture of a ferromagnetic nanowire at equilibrium is such that the magnetic moments are aligned along the wire axis. When the

wire is submitted to a strong external magnetic field in the opposite direction, it reverses the orientation of the magnetic moments. Depending of the shape and the material, this Magnetization Reversal Process can happen in different ways and the control of this process is fundamental for any potential applications of ferromagnetic nanowires, in particular for magnetic memories $[2, 3, 5]$.

The shape and the material of the nanowires strongly influence the nature of the Magnetization Reversal Process. In this work, two FM materials that show a different magnetic response were studied. Firstly, **nickel** nanowires were used to analyze how the aspect ratio influences the magnetic response. Then, **cobalt** nanowires were modelled to study the anisotropy of the magnetic response due to crystal structure. To study the interaction with the surrounding material, a core-shell structure of cobalt and **cobalt oxide** was modelled. For all the performed simulations, nanowires with length 1 μm and diameters in the range from 40 nm to 80 nm were used.

The system Co core and CoO shell permitted to analyze the **Exchange bias effect**. At the interface between the two materials there is a coupling of magnetic moments; at the macroscopic level, the main consequence of this coupling effect (Exchange bias) is the displacement of the Hysteresis Loop. With the developed Model it was possible to verify that the displacement is controlled by the strength of the coupling at the interface. It was also possible to observe that the Exchange bias is a surface effect, hence its efficacy depends on the ration interface/volume.

Acknowledgements

I would like to acknowledge that this work is not only the result of many hours of hard work from my side, but it is also the result of many inspiring conversations with my mentors. First, I want to thank my supervisors Marco and José at Universidad Politécnica de Madrid, that assisted me with the most difficult aspects of the *Object Oriented MicroMagnetic Framework* and guided me during this project. I am very grateful to them for giving me the opportunity to work at this project and for their patience and support in mentoring me. Also, I would like to thank Professor Rossi for being my supervisor at Politecnico di Torino and support me in the development of this work, even from distance. To professor Rossi I am also grateful for the helpful discussions and for the generous and wise advice during the final steps of this project.

Many thanks to Marco, Benedetta and Hunor for their precious and tireless help in the proofreading of this work. I feel so lucky to have your support and I cannot wait to return the favor.

My colleagues and friends both in Turin and in Madrid also deserve many thanks. During these years I have had many inspiring conversations, and it is thanks to them that I felt the excitement of being part of a community of learners.

I would like to thank my best friends, Giovanna, Alessio, Roberto, Simone, Gabriele, Alex, Marco, Andrea and Andrea. Thanks for your ability to turn big and stressful problems into small and solvable ones.

I am so grateful to my family, in particular to my parents for the support and encouragement they gave me since the first years of school, especially to my mum that has always believed in me, and to my sister for our study sessions and for all the indispensable conversations. To them I dedicate this thesis.

Table of Contents

1. Introduction: motivation for the study and thesis outline

Ferromagnetic nanostructures have attracted considerable attention due to their properties and possible applications. Nanowires are 1D nanostructure that exhibit an enhanced aspect ratio. This high value of shape anisotropy leads to unique magnetic properties and makes nanowires promising candidates for several applications [5, 6, 7].

For example in nanoelectronics, nanowires are promising candidates as recording media for the storage of information. In this field, a possible device that is currently studied is the **Racetrack memory**. That is a ferromagnetic nanowire in which the data are encoded as a pattern of bits that moves along the wire. As it is illustrated in figure 1.1, along this structure, the data '0' and '1' are made by magnetic domain and are generated through a current line (Data write pulse) and pushed by a Data drive pulse [5, 6].

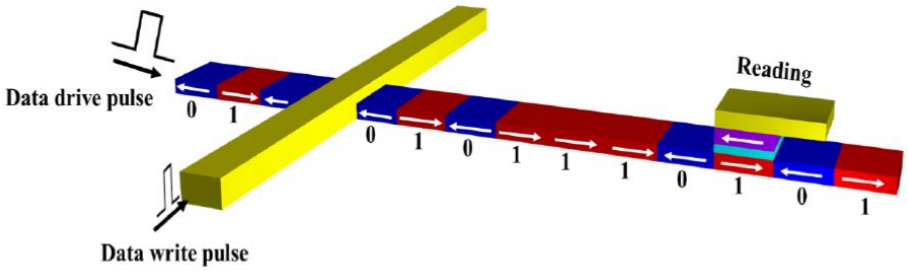

Figure 1.1 Illustration of a Racetrack memory. Magnetic domains of opposite magnetization form bits. The Data write pulse is applied through a current line. The bits are moved along the nanowire by a Data drive pulse, which is a spin-polarized current pulse injected into the nanowire. Information are read through a Reading head [6].

As a second application, it is worth mentioning that ferromagnetic nanostructures have witnessed increasing interest in biomedical applications. They can help the early detection of diseases like cancer, they act as contrast agents in imaging techniques like Magnetic Resonance Imaging, and they can be potentially used for cancer treatment by hyperthermia [7, 8].

For these applications, ferromagnetic nanostructures must be covered with biocompatible materials and functionalized with antibodies to interact specifically with cancer cells. The cancer cells, that internalized the nanostructures, are tagged with a magnetic nanoparticle

and can be observed and manipulated with an external magnetic field; we refer to this as **biolabeling**. Nanowires present high magnetic properties and this makes them promising candidates for biolabeling [7, 8].

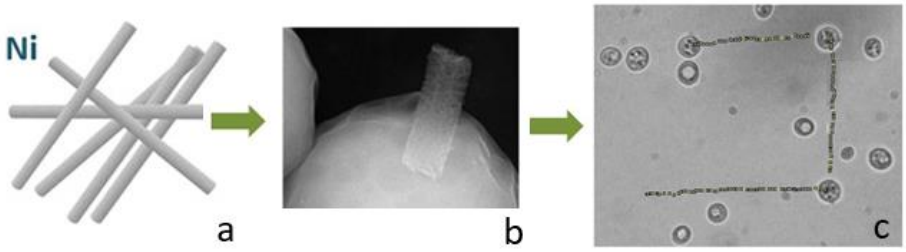

Figure 1.2 a) Illustration of Ni nanowires b) FE-SEM image of a yeast cell tagged with a Ni nanowire c) manipulation of tagged cells at the microscopic level via magnetic fields [8].

The shape and the material of the nanowires determine the macroscopic magnetic properties of the device. In the research and development of magnetic devices, computational micromagnetic simulations are a powerful tool that offers the possibility to compare the macroscopic magnetic response of different samples. Also, with computational micromagnetics it is possible to observe the magnetic moments distribution inside the sample, at a microscopic level, useful to understand the Magnetization Reversal Process of a sample.

The purpose of this study was to develop a Model to simulate the magnetic response of a ferromagnetic nanowire and perform some 3D micromagnetic simulations to investigate the influence of material parameters and geometry on the macroscopic magnetic response and on the magnetic moments distribution along the sample.

The interaction with the surrounding material is also important to understand the overall magnetic behavior of a device. With the model, we aimed to study the Exchange Bias, a surface effect that happens when a ferromagnetic (FM) and an antiferromagnetic (AFM) material are coupled at their interface.

To this end, before presenting the model and the simulation results, this work introduces some theoretical aspects, useful to understand the physics involved in the real material

system and involved in the micromagnetic model. In **Chapter 2**, basic principles of micromagnetism, the energetics of magnetic interactions and the working principles of micromagnetic computational simulations are presented.

During this work, I made use of the micromagnetic simulation program OOMMF, shorter for Object Oriented MicroMagnetic Framework, an open source program written in C++ [4]. The input for the program is a configuration file that describes sample materials and shape and defines the simulation conditions.

The first task of this thesis project was to write the configuration file to model a ferromagnetic nanowire. In order to study the Exchange Bias effect, the second step was to write a configuration file to simulate a more complex structure, made of a ferromagnetic core and an antiferromagnetic shell. In **Chapter 3**, it is presented the developed Model for the simulation of a ferromagnetic nanowire and the improvements that have been made to study the interaction with the surrounding material (Exchange Bias effect).

In **Chapter 4** the simulation results are presented. Ferromagnetic nanowires of different geometries, different materials, and with different simulation conditions have been simulated, with the aim to analyze their different magnetic response and texture.

The first investigated parameter has been the **aspect ratio**. Nickel nanowires of constant length were used to show the correlation between wire diameter and magnetic response. It was possible to observe that the type of Magnetization Reversal Process of a Ni nanowire depends on the wire diameter.

The **crystal structure** was the second parameter analyzed. In this case a cobalt wire has been used, and three simulations were performed by changing the easy axis direction for the magnetization. Cobalt is a FM material in which the magnetization is dominated by the competition between shape and orientation of the crystal structure (Magnetocrystal Anisotropy). It was possible to observe that for a Co nanowire the Magnetocrystal Anisotropy strongly influences the shape of the Hysteresis loop.

During a simulation, the modelled sample is discretized and is divided into equal sized parallelepipeds called cells. Along this work, a study of the influence of the **cell size** on simulation results is presented.

When an AFM material covers the surface of the FM wire, the magnetic moments of the two materials are coupled at the interface (**Exchange Bias effect**). At the macroscopic level, the main consequence is the displacement of the Hysteresis loop. During this work we performed a study on the FM-AFM coupling on a wire made by a Co core and a CoO shell. Using the model, we were able to verify that the displacement is controlled by the strength of the coupling at the interface. It was also possible to verify that the Exchange Bias is a surface effect, hence its efficacy depends on the ratio interface/volume.

A conclusion based on all the considered aspects has been formulated at the end of the thesis, in **Chapter 5**.

2. Theoretical background: basic principles of micromagnetism, energetics of magnetic interactions and computational micromagnetics

In this chapter, some important concepts and parameters regarding ferromagnetic nanowires and the phenomenon of exchange bias are discussed. The magnetic interactions and their influence on the energy of the system are analyzed by energy minimization considerations. A brief description of the working principle of a micromagnetic simulation is also presented at the end of this chapter.

2.1 Microscopic origin of magnetism

The origin of magnetism in a material can be identified at the atomic scale; in an atom, the magnetic moment derives from the angular momentum of its electrons. Each atomic electron presents two types of angular momenta: an **orbital moment** $\boldsymbol{L}$, that derives from the electron orbital motion, and a **spin momentum** $\boldsymbol{S}$; although the electron is an elementary point particle, for the spin momentum an analogy with the spin of a rigid body can be made [6, 9].

The magnetic moment of free atoms $\boldsymbol{\mu}$ can be expressed as follows:

Equation 2.1.1 [10]

$$\boldsymbol{\mu} = -g\mu_B(\boldsymbol{L} + \boldsymbol{S})$$

where g is the generalized Landè factor (approximately $g = 2$), $\mu_B$is the Bohr magneton ($\mu_B = 9.2741 \cdot 10^{-24}\ \mathrm{A \cdot m^2}$), $\boldsymbol{L}$ is the orbital momentum and $\boldsymbol{S}$ is the electron spin.

In a solid, the spin of unpaired electrons is the largest contribution to the magnetism in an atom [10]. In a crystal lattice, the atomic magnetic moments of neighboring atoms interact with each other. The four main types of atomic interactions in ferromagnetic (and antiferromagnetic) materials, are presented in the chapter *2.6 Energetics of magnetic interactions and equilibrium state.*

To perform micromagnetic simulations, instead of considering individual magnetic moments $\boldsymbol{\mu}$, a continuous magnetization function $\boldsymbol{M}$ is used to approximate the atomic interactions. The magnetization $\boldsymbol{M}$ is the local average density of magnetic moments and it can be expressed as follows:

Equation 2.1.2 [10]

$$\boldsymbol{M}(\boldsymbol{r}) = \frac{1}{V}\sum_{i} \boldsymbol{\mu_i}$$

In comparatively small systems, for example a cube of 5 nm length, the number of atoms is large. Assuming a cubic structure of Co or Ni (with a lattice spacing of 2.5 Å), in the cubic system of 5 nm length there are $8 \cdot 10^3$ atoms. If the average of magnetic moments $\boldsymbol{\mu_i}$ is performed over the appropriate scale, it will always contain a sufficiently big number of magnetic moments and the continuous approximation is valid $[10]$.

Domains and domain walls

In magnetic materials, the magnetic moments of atoms are forced to align with one another and to point in the same direction by an internal short-range interaction called **exchange interaction**. The nature of exchange interaction defines the type of magnetism: if the interaction promotes a parallel alignment of magnetic moments, it produces a long-range ferromagnetic (FM) order; if the interaction favors an antiparallel alignment of magnetic moments, it induces an antiferromagnetic (AFM) order $[6]$.

From a macroscopic point of view, a parallel alignment of magnetic moments gives rise to a net magnetization of the sample, able to attract other magnetic materials. However, FM bulk materials in nature show zero external magnetization and they generally do not exert any attractive or repulsive force on other magnetic materials. This is because the structure of bulk ferromagnetic materials is typically divided into small regions called magnetic domains. A domain is a region of uniform magnetization where the magnetic moments are aligned; a boundary between domains is called Domain wall. The formation of domains avoids the presence of a magnetic field around the material, minimizing the energy of the system and minimizing the attraction of other magnetic materials $[11]$.

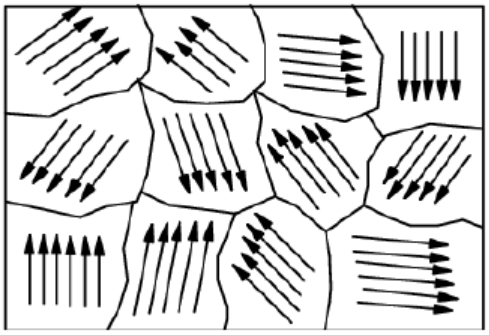

Figure 2.1.1 Schematic representation of a Ferromagnetic material divided into domains. Inside domains the magnetic moments are aligned, but the net magnetization of the sample is 0 [11].

In other words, in ferromagnetic materials, the exchange interaction aligns all spins in the same direction at a microscopic scale, but this alignment is not preserved macroscopically between domains. The alignment of domains is possible when an external magnetic field is applied.

2.2 Hysteresis loop

When a ferromagnetic body is submitted to an external magnetic field ($\boldsymbol{H}$) along one direction, it magnetizes, this means that in the sample the magnetic moments of the atoms tend to align with the external field. This configuration is described by the magnetization vector $\mathbf{M}$, a continuous function of the position representing the spatial density of the magnetic moments [9].

If the external magnetic field is big enough, the ferromagnetic material will eventually reach its magnetization saturation (M_S), that is the configuration in which all the magnetic moments are oriented along the field direction.

In figure 2.2.1 it is reported a typical hysteresis loop. The unit magnetization vector ($\boldsymbol{m}$), which is the ratio $\boldsymbol{M}/M_S$, is plotted as a function of the applied field ($\boldsymbol{H}$). Both the unit magnetization vector and the external field are vectors so, in order to obtain a hysteresis loop, on the y axis it is generally plotted the value of the unit magnetization vector along a specific direction, for example the direction of the applied external field ($m_{\parallel}$), and on the x axis it is plotted the magnitude of the applied external field (H).

If the external field is removed, typically the material does not reach the demagnetized configuration. Part of the magnetization will remain in the material; this state in the $m_{\parallel}(H)$ plane corresponds to a point (called remanence) on the vertical axis $[0, M_r]$. To reach the condition $m_{\parallel}$=0, a negative field must be applied and the corresponding point on the $m_{\parallel}(H)$ plane along the horizontal axis $[-H_C, 0]$ is called coercivity. If the negative magnetic field is increased in magnitude the material reaches its negative magnetic saturation (-M_S). If H is then brought to 0 and then increased again in the positive direction, the material will firstly reach its negative remanence, then the positive coercivity and finally the magnetic positive saturation again [12].

For samples that show a symmetric hysteresis loop, the two values of magnetization saturation, the two values of remanence and the two values of coercivity are equal in magnitude and opposite in sign, as is shown in figure 2.2.1, while this is not true in other cases, for example for samples showing exchange bias effect.

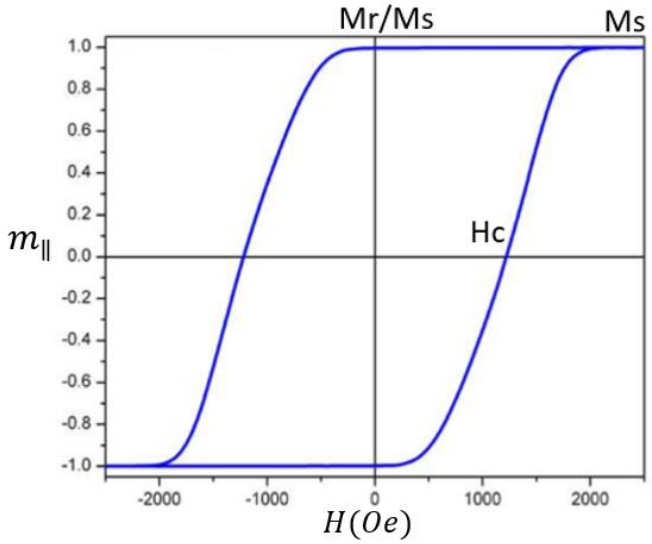

*Figure 2.2.1 Hysteresis loop of a typical ferromagnetic bulk material. $m_{\parallel}$ is the z component of the unit magnetization vector **m** (**m**=**M**/M_S), plotted as a function of applied field **H** (Oe) along z. Ms is the magnetization saturation, Mr/Ms is theremanence, Hc coercivity* [11].

2.2.1 Influence of geometry on the hysteresis loop

In a magnetic material, typically, there is a directional dependence of the magnetic response that is a preferred direction for the magnetization vector (**easy axis**). This phenomenon is called magnetic anisotropy.

There are several types of magnetic anisotropy; the one related to the geometrical shape of the sample is called **shape anisotropy.** It plays a crucial role in the magnetization of a nanowire. When a sample of nanometric dimensions is not spherical, the bigger dimension becomes an easy axis for the magnetization, that is a preferred direction for the magnetization vector.

Another term related to the geometry and crucial at the nanoscale is the **surface anisotropy** that emerges because of the break of lattice periodicity at the surface.

In nanowires, the shape and the surface are sources of enhanced anisotropy in the magnetization. The magnetic moments in a nanowire prefer to be aligned along the wire axis and the magnetization configuration is typically a **single domain**, with the magnetic moments aligned along the wire axis, in one of the two orientations. When the wire is submitted to a magnetic field ($\boldsymbol{H}$) in the opposite direction, if the field is big enough (**Reversal field**), along the wire starts the **reversal mechanism**. At that magnitude of external field, the magnetic moments reverse orientation; the resulting hysteresis loop typically presents a **squared shape.** In figure 2.2.1.1 is shown a hysteresis loop for a single nanowire simulated with the program OOMMF.

The reversal mechanism in a ferromagnetic nanowire can occur in different ways. In the paragraph *2.4 Magnetization reversal modes*, the reversal mechanism is described with more details.

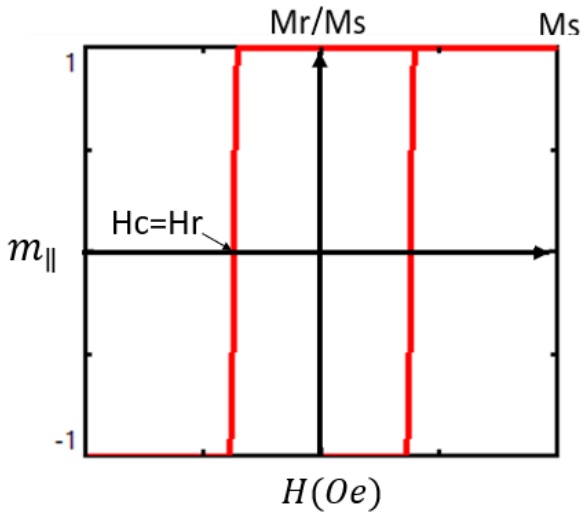

*Figure 2.2.1.1 Typical hysteresis loop of a ferromagnetic nanowire. $m_{\|}$ is the z (wire axis) component of unit magnetization vector **m** (**m**=**M**/M_S), plotted as a function of applied field **H** (Oe) along z (wire axis).*

2.3 Material parameters

In a crystal lattice there is a directional dependence of the magnetic response; this phenomenon is called magnetic anisotropy. Among the terms describing the anisotropy of a ferromagnetic sample, the **magnetocrystalline anisotropy** is a material property. This type of magnetic anisotropy is determined by the crystal structure and it results in a variation of the magnetic properties of the material depending on the orientation with respect to the crystallographic structure [12].

The magnetocrystalline anisotropy is one of the magnetic interactions that define the total magnetization of a sample. The intensity of this interaction is different for each material. The material parameter that describes the strength of the magnetocrystalline anisotropy is called anisotropy constant $K(\mathrm{J/m^3})$.

In table 2.3.1 the anisotropy constants of nickel and cobalt are compared. The values are the default values of the OOMMF microsimulation program that have been used for the simulations [4]. In the program, a positive value indicates that the material presents an easy axis for the magnetocrystalline anisotropy while a negative value indicates that the material

presents an easy plane. It can be noticed that Ni presents an easy plane while Co an easy axis, and by comparing the absolute value of K it is possible to observe that Co shows a more intense magnetocrystalline anisotropy than Ni.

Table 2.3.1 [4]

Material	**Anisotropy Constant K $(\mathbf{kJ/m^3})$**
Ni	-5,7
Co	520

In nanowires of Co, the crystal anisotropy can be comparable in strength to shape anisotropy. Therefore, the magnetization behavior in these nanostructures is dominated by competition between shape anisotropy and magnetocrystalline anisotropy $[13]$. On the contrary, in nanowires of Ni the magnetocrystalline anisotropy is negligible with respect to the shape anisotropy.

The phenomenon called **exchange interaction** is another type of magnetic interaction that participates in the magnetization of a sample. This interaction between magnetic moments favors their alignment and is the main interaction for ferromagnetic materials at the nanoscale. As for the magnetocrystalline anisotropy, the strength of the exchange interaction is a material property. The material parameter that describes its intensity is called exchange constant $A(\mathrm{J/m})$.

In table 2.3.2 the exchange constants of Ni and Co are compared. The values are the default valued of OOMMF microsimulation program that have been used for the simulations. It can be noticed that Ni presents a smaller value for exchange constant, therefore in a Ni sample the magnetic moments are less inclined to remain parallel than in Co.

Table 2.3.2 [4]

Material	**Exchange Constant *A* $(\mathbf{pJ/m})$**
Ni	9
Co	30

When a ferromagnetic sample is submitted to a magnetic field $\boldsymbol{H}$, if the field is strong enough the sample reaches a configuration in which all the magnetic moments are oriented along the field direction. This configuration is called **magnetization saturation** $M_S(\mathrm{A/m})$ and is a material property.

In the table 2.3.3 the magnetization saturation of Ni and Co are compared.

Table 2.3.3 [4]

Material	***Magnetic saturation M_S $(\mathbf{kA/m})$***
Ni	490
Co	1400

The last material parameter that is important to present is the **exchange length**. For the description of the Reversal Process of ferromagnetic nanowires, this parameter is of primary importance because it governs the width of the transition between magnetic domains (domain wall). It is also a crucial parameter in the design of a micromagnetic simulation; in the definition of the mesh, the exchange length provides a quantitative measure for the mesh resolution; this aspect will be better explained in the chapter 2.7 *Computational Micromagnetics in OOMMF*.

The exchange length can be derived by the exchange anisotropy and magnetization saturation as in equation 2.3.1. Where the constant $\mu 0$ is the permeability of free space.

Equation 2.3.1 [2, 14]

$$l_{ex} = \sqrt{\frac{A}{\mu 0 * Ms^2/2}}$$

The exchange length of Ni results as follows:

Equation 2.3.2

$$l_{ex\_Ni} = \sqrt{\frac{9 * 10^{-12}[N]}{4\pi * 10^{-7} * (490 * 10^3)^2/2\,[N/m^2]}} = 7.7 * 10^{-9}\,m$$

And the exchange length of Co results as follows:

Equation 2.3.3

$$l_{ex\_Co} = \sqrt{\frac{30 * 10^{-12}[N]}{4\pi * 10^{-7} * (1400 * 10^3)^2/2\,[N/m^2]}} = 4.9 * 10^{-9}\, m$$

2.4 Magnetization reversal modes

At equilibrium, the magnetization configuration of nanowires and nanotubes is such that all the magnetic moments aligned along a common direction. This configuration is called **single domain**. When the wire is submitted to an external magnetic field in the opposite direction, if the magnetic field is intense enough, the wire changes the magnetization configuration. For ferromagnetic nanostructures, this magnetic reversal process can happen in different modes. For example, in figure 2.4.1 the possible magnetization reversal modes in a magnetic nanotube are represented [15]. The magnetization reversal can occur by a coherent rotation of all moments or by the nucleation and movement of a domain wall, that can be vortex type or transverse type.

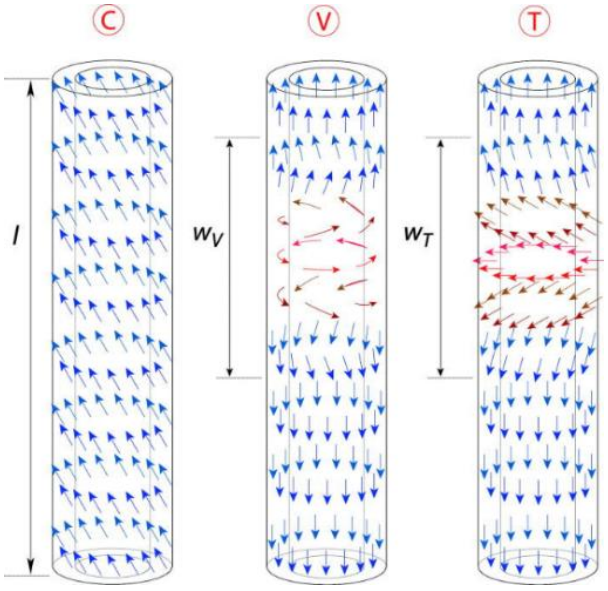

Figure 2.4.1 Types of domain walls in ferromagnetic nanotubes. Left: coherent reversal mode. Center: vortex reversal mode, with a domain wall of thickness, w_V. Right: transverse reversal mode, with a domain wall of thickness, w_T. [15].

In nanowires, a coherent rotation of magnetic moments can occur for diameters smaller than a critical dimension. In the study [16] the authors proved that the threshold diameter is close to the exchange length value of the material. Other studies [2, 17] performing simulations on ferromagnetic nanowires have shown that, above the threshold diameter, the reversal occurs through the nucleation and propagation of a Domain Wall (DW). The DW can be one of the two types presented for nanotubes, transverse type or vortex type. The geometry and the material parameters of the nanowire influence the type of domain wall.

During this study, by performing different simulations with different conditions, it was possible to explore the dynamic of domain wall nucleation and propagation along a ferromagnetic nanowire. In figure 2.4.2 for example, the reversal process on a cobalt nanowire of diameter 40 nm is represented. At the two basis of the wire, two transverse DWs nucleate and then propagate along the wire. During this process, the magnetic configuration of the wire is made by more than one domain, separated by the domain wall.

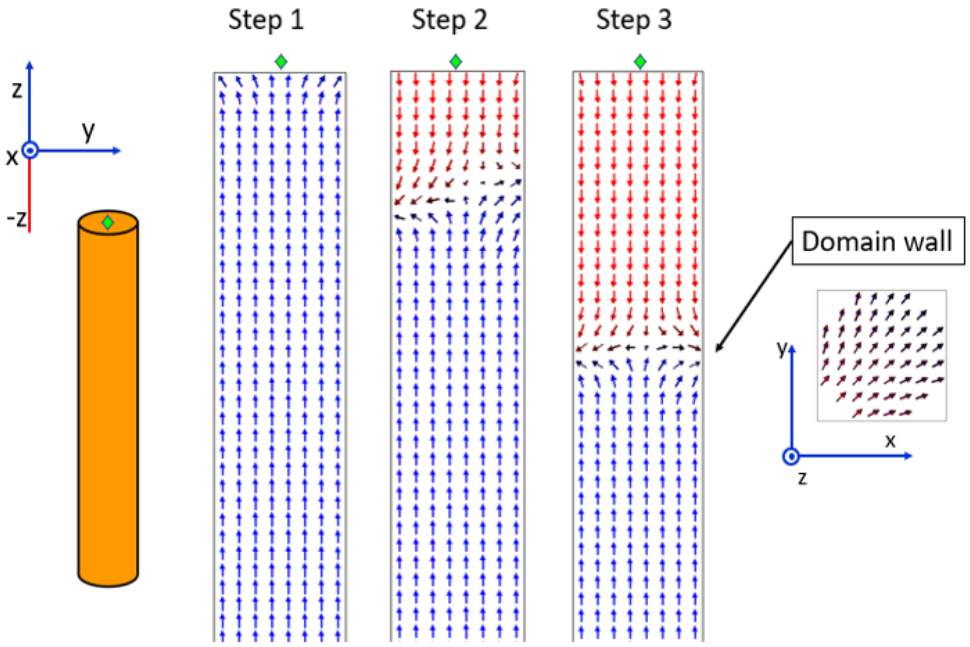

Figure 2.4.2 A scheme of the magnetization reversal process of a Co nanowire. The magnetization vector has been represented with the program OOMMF. The software divides a cylindric nanowire into cells, the orientations of the magnetization vector in each cell is represented by an arrow. The green rhombus is used to indicate the position of the cylinder base.

2.5 Exchange bias effect

The **exchange bias** is a surface effect that can be obtained with an Antiferromagnetic (AFM) material facing a ferromagnetic (FM) material. At the interface, a new exchange interaction keeps the magnetic moments of the FM parallel to the magnetic moments of the AFM material. This coupling results in a shift of the hysteresis loop.

Figure 2.5.1 shows a schematic representation of a FM/AFM bilayer at two different stages of the hysteresis loop. When the magnetic moments of the ferromagnetic material are parallel to the closest magnetic moments of the AFM material, the system is in a stable configuration and a strong external magnetic field is necessary to change the magnetization of the FM material. On the contrary, when the magnetic moments of the FM material are antiparallel to the closest magnetic moments of the AFM layer, the system is not in the configuration of minimum energy, and a small external field is required to change the magnetization of the FM material.

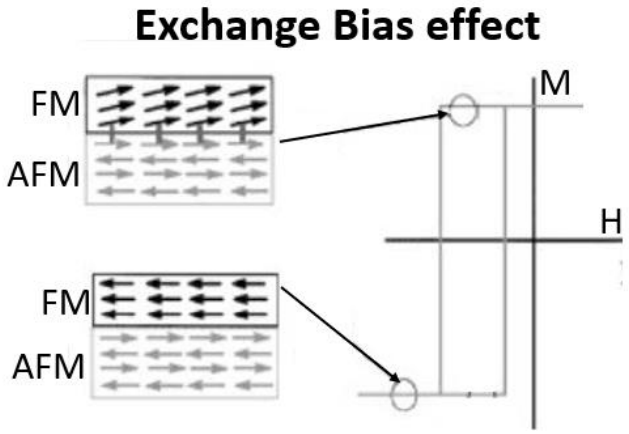

Figure 2.5.1 A schematic representation of a FM/AFM bilayer at different stages of an exchange-biased hysteresis loop. FM stands for ferromagnetic and AFM stands for antiferromagnetic [18].

The exchange bias phenomenon is of fundamental utility in magnetic devices, for example it is used in the reading heads of hard disks, where the coupling between the FM and AFM layers allows to obtain a magnetic sensor that shows its maximum sensibility at very small magnetic fields [19, 20].

2.6 Energetics of magnetic interactions and equilibrium state

As briefly mentioned in previous paragraphs, bulk ferromagnetic material forms domains (and domain walls) to reduce the magnetic field around the sample and to minimize the total energy of the system.

The magnetization state of a magnetic material at equilibrium always arises from energy minimization considerations. Several magnetic interactions, that depend on the magnetic material and on the sample geometry, compete to determine the equilibrium magnetization of a sample. The main magnetic interactions are described in the following subchapters.

As mentioned in the chapter *2.1 Microscopic origin of magnetism*, to perform micromagnetic simulations, the energy terms that describe the atomic interactions are not expressed as a function of individual magnetic moments $\boldsymbol{\mu_i}$, but as a function of the magnetization $\boldsymbol{M}$ (the local average density of magnetic moments) or as a function of the unit magnetization $\boldsymbol{m} = \boldsymbol{M}/M_s$. It is important to notice that $\boldsymbol{M}(\boldsymbol{r})$ and $\boldsymbol{m}(\boldsymbol{r})$ are continuous and differentiable functions. This allows to express some magnetic energy terms, that will be presented in following subchapters, using differential operators. The resulting equation for the total energy can be solved numerically [10].

2.6.1 Exchange interaction

The exchange interaction is the phenomenon that favors parallel (or antiparallel) alignment of the magnetic moments in ferromagnetic (or antiferromagnetic) materials. It is a short-range phenomenon that is only effective between the neighbor atoms.

In the continuum limit, the exchange energy can be then expressed with an integral over the volume as in the following expression:

Equation 2.6.1.1 [9, 10]

$$E_{ex} = A \int_V \left[(\nabla m_x)^2 + \left(\nabla m_y\right)^2 + \ (\nabla m_z)^2 \right] d^3r$$

Where A is the exchange contant and m_x, m_y, m_z are the cartesian components of the unit magnetization vector. It must be noticed that the exchange energy depends on the spatial derivative of the magnetization, a feature that is used in numerical methods for the simulation of ferromagnetic samples [9].

2.6.2 Magnetocrystalline anisotropy

The symmetry of the crystal structure affects the spatial distribution of the orbitals of the magnetic atoms. In FM materials, the magnetic moments are usually forced to align along a specific crystallographic axis, called **easy axis.** In the case of hexagonal crystal, for example bulk Co, the hexagonal axis is the direction of easy magnetization [6].

The magnetocrystalline anisotropy is mainly due to the coupling spin-orbit of the electrons. When an external field is applied, it tries to re-orient the spin, and this would also result in the re-orientation of the orbit. But the orbit is strongly coupled with the lattice and therefore there is a resistance that is necessary to overcome to rotate the spin [6].

As for the exchange energy, also the magnetocrystalline anisotropy energy can be expressed as a function of the magnetization $\boldsymbol{m}(\boldsymbol{r})$, i.e. a continuous and differentiable function. As the energy cost associated with magnetocrystalline anisotropy depends on the type of crystal structure, the function takes a different expression for each crystal lattice. In a general form it can be expressed as follows:

Equation 2.6.2.1 [9, 10]

$$E_{anis} = \int_V f_{anis}(\boldsymbol{m})\, dV$$

For cobalt, for example, the function takes the following expression:

Equation 2.6.2.2 [10]

$$f_{anis}(\boldsymbol{m}) = -K_1 cos^2(\theta) + K_2 cos^4(\theta)$$

where θ is the angle between the magnetization $\boldsymbol{m}$ and the easy axis. $K_1$and K_2 are exchange constants for the material; as mentioned in the paragraph 2.1 *Materials*

Parameters, the exchange constant can have a positive or a negative value; when $K_1 > 0$ the axis is an easy axis for the magnetization, when $K_1 < 0$ the axis becomes hard (which produces an easy plane).

2.6.3 Zeeman interaction

The Zeeman interaction represents the energy cost of misalignment between magnetization vector and the applied magnetic field. This energy term can be expressed as follows:

Equation 2.6.3.1 [9]

$$E_{Zeeman} = -\mu_0 \int_V \boldsymbol{M}(\boldsymbol{r}) \cdot \boldsymbol{H_{ext}} dV$$

where μ_0 is the permeability of vacuum, $\boldsymbol{M}(\boldsymbol{r})$ is the magnetization and $\boldsymbol{H_{ext}}$ is the applied external magnetic field.

The Zeeman energy is minimized when all the local magnetic moments are aligned along the direction of the external magnetic field. In the continuous limit, the energy is considered minimized when the magnetization vector is aligned with the external field.

2.6.4 Magnetostatic interaction (demagnetizing field)

The presence of an external magnetic field results not only in the magnetization of the ferromagnetic sample, it also creates a magnetic field inside and outside the bulk, pointing in the opposite direction to the magnetization. This field is called demagnetizing field, as the term indicates its tendency to act on the magnetization in a way that reduces the total magnetic moment.

The demagnetizing field is created because the magnetic moments at the surface create free magnetic charges called magnetic poles, that generate a closed magnetic field between them ($\boldsymbol{H}_{demag}$). As a result, the magnetic field $\boldsymbol{B}$ (the flux density) inside the ferromagnetic material is different from the magnetization field $\boldsymbol{M}$, as it can be seen in figure 2.6.4.1.

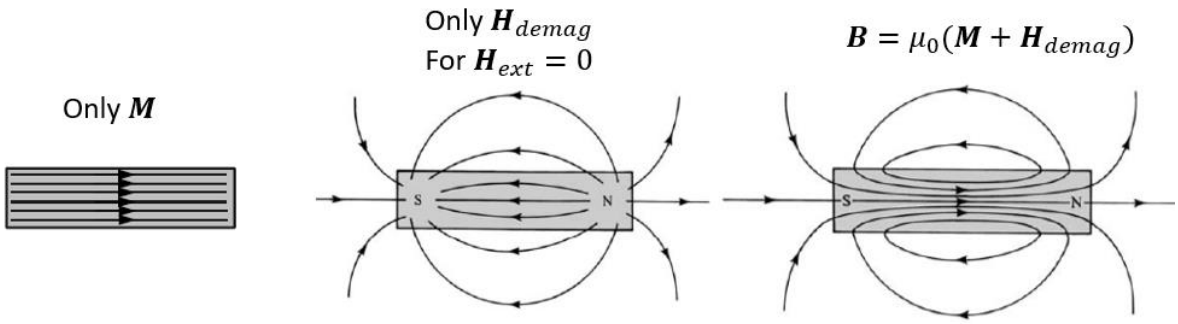

Figure 2.6.4.1 Comparison of magnetization $\boldsymbol{M}$, demagnetizing field $\boldsymbol{H}_{demag}$, and flux density $\boldsymbol{B}$, inside and outside a ferromagnetic material [11].

The demagnetizing energy is the responsible for the formations of domains and domains walls in bulk ferromagnetic materials. In the continuum limit, the Demagnetizing energy can be express as follows:

Equation 2.6.4.1 [9]

$$E_{demag} = \frac{1}{2}\mu_0 \int_V \boldsymbol{H_{demag}}(\boldsymbol{r}) \cdot \boldsymbol{M}(\boldsymbol{r})\, dV$$

where $\boldsymbol{M}(\boldsymbol{r})$ is the magnetization and $\boldsymbol{H_{demag}}(\boldsymbol{r})$ is a function that contributes to the divergence of the magnetization when some magnetic poles are present at the surface.

The demagnetizing field is a function of the position that derives from the interaction of all magnetic vectors with each other, therefore computing the demagnetizing energy is the most expensive part of any micromagnetic simulation.

2.6.5 Total magnetic energy

The total energy of the sample can be described as the sum of the energy terms described in previous subchapters.

In its integral form, the total energy E is a function of the magnetization vector field $\mathbf{M}$ (or the unit magnetization vector field $\boldsymbol{m} = \boldsymbol{M}/M_S$) as given by equation 2.6.5.1:

Equation 2.6.5.1 [3, 4, 9]

$$E(\boldsymbol{M}) = \int \left(A * (\boldsymbol{\nabla}\mathbf{m})^2 + f_{anis}(\boldsymbol{m}) - \mu_0\, \boldsymbol{M} \cdot \boldsymbol{H}_{ext} + \tfrac{1}{2}\boldsymbol{M} \cdot \boldsymbol{H}_{demag}(\boldsymbol{r}) \right) dV$$

The first term inside the integral is the energy expression for the exchange interaction, that depends on the spatial derivative of magnetization. A is the exchange constant (J/m), a material parameter describing the strength of the exchange interaction.

The second term is the magnetocrystalline anisotropy energy. The function of the unit magnetization vector $f_{anis}(\boldsymbol{m})$ takes a different expression for each crystal lattice.

The third term describes the Zeeman energy, the energy corresponding to the misalignment between magnetization $\mathbf{M}$ and external field $\boldsymbol{H}_{ext}$.

The last term concerns the energy contribution of magnetostatic interactions. $\boldsymbol{H}_{demag}$ is the demagnetizing field and it is a function of the unit magnetization vector field $\boldsymbol{m}$.

The derivative of the total energy E with respect to the magnetization $\mathbf{M}$ is a vector field which is also defined by the contribution of the Exchange interaction, the Magnetocrystalline anisotropy, the Magnetostatic interaction and the Zeeman interaction. This vector field is called effective field $\boldsymbol{H}_{eff}$ and is given by the expression 2.6.5.2:

Equation 2.6.5.2 [3, 4, 10]

$$\boldsymbol{H}_{eff} = -\frac{1}{\mu_0}\frac{\partial E}{\partial \boldsymbol{M}}$$

A sample reaches the magnetization configuration of the minimum energy. Therefore, the **equilibrium state** is reached when:

Equation 2.6.5.3 [4]

$$\boldsymbol{M} \times \boldsymbol{H}_{eff} = 0$$

If a sample is not in the equilibrium it evolves to reach it. The equation describing the evolution of magnetization in time is an Ordinary Differential Equation (ODE) called Landau–Lifshitz–Gilbert (LLG) equation and has the expression:

Equation 2.6.5.4 [3, 4]

$$\frac{d\boldsymbol{M}}{dt} = -|\bar{\gamma}|\, \boldsymbol{M} \times \boldsymbol{H}_{eff} - \frac{|\bar{\gamma}|\alpha}{M_S}\boldsymbol{M} \times \left(\boldsymbol{M} \times \boldsymbol{H}_{eff}\right)$$

The first term on the right side of the equation describes the fact that if there is an angle between magnetization and effective field there is also a torque on the magnetization; the time evolution of the magnetization field is proportional to the torque, the constant of proportionality ϒ (m/A*s) is called gyromagnetic ratio. The corresponding motion of the magnetization is a precession around the effective field, as it is shown in figure 2.6.5.1 (a).

The second term describes the energy losses and the local dissipative phenomena that prevent the precession to continue indefinitely. The constant α (dimensionless) is the damping constant. The presence of dissipative phenomena results in a damping of the magnetization which brings it in the direction of the effective field, as shown in figure 2.6.5.1 (b).

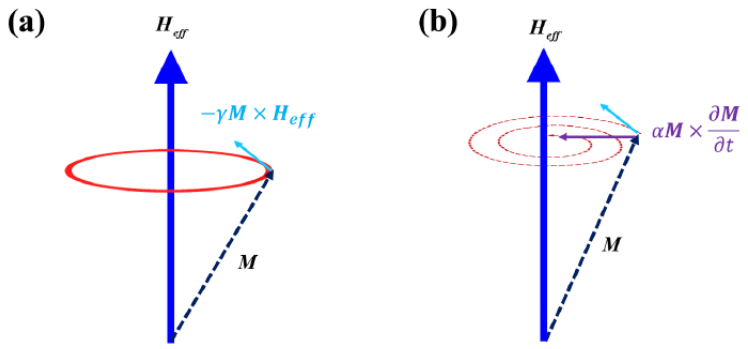

Figure 2.6.5.1 Schematic representation of the magnetization precession around the effective magnetic field, (a) in the absence of energy losses, (b) with energy losses that results in a damping of the precession [6].

2.6.6 Effect of temperature

The LLG equation and the equation of the total energy are strictly exact only at absolute zero temperature ($T = 0\ K$) [4, 10].

The effects of temperature on magnetization dynamics are important for various research topics, as, for example, heat assisted magnetic recording [21]. To include temperature effects in micromagnetic simulations, at constant temperatures, one possibility is to adjust material parameters according to their temperature dependence; for example the magnetization saturation is a function of temperature ($M_S(T)$), and at non-zero

temperature the exchange length might be expressed in terms of $M_S(T)$ as in equation 2.6.6.1.

Equation 2.6.6.1

$$l_{ex} = \sqrt{\frac{A}{\mu 0 * (Ms(T))^2 / 2}}$$

During this study, to perform micromagnetic simulations on ferromagnetic nanowires, two materials have been used: nickel and cobalt; the default values of the simulation program OOMMF have been used for material parameters. In chapter 4 (simulation results), the last paragraph deals with some energy considerations. In paragraph *4.7.1 Energy considerations*, the demagnetizing energy is compared to the thermal energy; it is possible to see that room temperature can be considered a low temperature for this system, thus the LLG and energy equations are valid at that temperature.

2.7 Computational Micromagnetics in OOMMF

The 3D micromagnetic calculation of the software OOMMF makes use of the finite difference method (FDM), which requires the discretization of the sample. The method divides the sample into parallelepipeds of identical volume named cells [4] and then considers physical properties as constant inside each cell, for example with this method the total magnetization is a step function, as its value is constant inside each single cell and it can be different between cells.

The dimension of cells is a crucial parameter. Its importance during a micromagnetic simulation is twofold. The first aspect to consider is that during the simulation of rounded objects there is an error associated with the **staircase discretization** of the object. The simulation results are influenced by dimension of cells (by the mesh resolution); a smaller cell size allows to better resolve a curved geometry [22]. For example, figure 2.7.1 shows how difficult it is to resolve a sphere geometry with cells that are too big and demonstrates the effect of altering the number of cells in a rounded geometry.

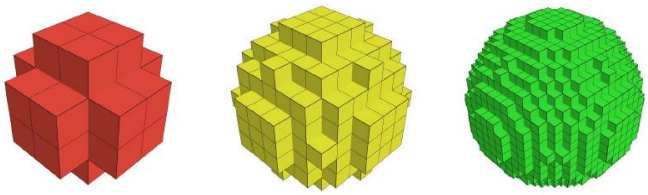

Figure 2.7.1 Approximation of the shape of a sphere by cubes [10].

The second aspect to consider is that within a micromagnetic simulation, each cell is homogeneously magnetized. This means that the atoms inside a cell are considered aligned during all the simulation. If cells are sufficiently small, this is an acceptable assumption because at an atomic scale the exchange interaction is the most significant energy term [10]. The exchange length is the material parameter that defines the length scale over which the direction of magnetization does not change significantly. For this reason, to perform micromagnetic simulations, it is important to fix the cell side to be equal or smaller than the exchange length.

By considering these two aspects, a smaller cell size leads to a better simulation. However, to establish the dimension of the cells for a simulation, the computational cost should be considered as well. By making the mesh *n* times as fine, then the number of the cells in the simulation increases by n^3 (since the system is three-dimensional) and this results in a massively increase of computational costs [10].

2.7.1 Evolution of magnetization

The software OOMMF offers two ways to find the stable magnetization configuration of a sample. One possibility is to perform an energy minimization simulation; in this case the magnetic state advances by obeying to direct energy minimization methods. It is necessary to specify a tolerance for the discrepancy of the two vectors, magnetization ($\mathbf{M}$) and effective field ($\boldsymbol{H}_{eff}$). When the difference between these two vectors is under the tolerance, the system has reached the equilibrium state. The other possibility is to perform a dynamic simulation in which the magnetic state advances from an initial configuration obeying to LLG dynamics; in this case the ODE solver of OOMMF integrates the LLG differential equation (equation 2.6.5.1) repeatedly [4].

3. Nanowire Model: a description of the developed code for the simulation of ferromagnetic nanowires

To study the magnetic response of some ferromagnetic nanowires I made use of the micromagnetic simulation program OOMMF (Object Oriented MicroMagnetic Framework) [4]. The input for the program is a **Configuration file** that is a text file written in the Tcl syntax, a programming language that allows to define spatially distributed fields and their change over time in an easy way.

This configuration file, that will be read by the simulation tool at run time, is used to describe the sample materials and shape, and to define the simulation conditions.

The first task of this thesis-project was to write the configuration file to obtain the Hysteresis loop of a ferromagnetic nanowire. This allowed to perform some simulations on nanowires of nickel and cobalt that can be fund in Chapter *4. Simulation results*. To study the interaction with the surrounding material, the second step was to create a configuration file to simulate and study a more complex structure, made of a ferromagnetic core and an antiferromagnetic shell. This structure can be used, for example, to describe a ferromagnetic cobalt wire, that is oxidized on the surface, creating a layer of cobalt oxide (CoO).

In this chapter the configuration files for the first and the second task are presented, with a particular focus on the improvements that have been made to describe a core-shell system.

3.1 Configuration file for simulate the Hysteresis loop of a ferromagnetic nanowire

The Tcl code presented in this paragraph simulate Hysteresis loop of a cylindrical nanowire. The following code is reported as a picture, while the text of the code can be found at the end of this work, in the chapter *6. Appendix Tcl code files*.

In the following lines of the code, some constants for later use and materials parameter are defined. In particular, the magnetization saturation, the exchange constant and the anisotropy constant of nickel and cobalt are defined.

```
# MIF 2.1
# DESCRIPTION: Hysteresis loop of a cylindrical nanowire ####################
# In this file is possible to change some parameters     ####################
# to understand their influence on the hysteresis loop   ####################
########## CONTANTS ############################################################

set pi [expr {4*atan(1.0)}]
set mu0 [expr {4*$pi*1e-7}]; #[N/A^2]

### MATERIAL PARAMETERS: default value of Co and Ni for OOMMF ##############

set Ms_Co 1400e3; #saturation magnetization [A/m]
set A_Co 30e-12; # exchange constant [J/m]
set K_Co 520e3; # anisotropy constant [J/m^3]

set Ms_Ni 490e3; #saturation magnetization [A/m]
set A_Ni 9e-12; # exchange constant [J/m]
set K_Ni -5.7e3; # anisotropy constant [J/m^3]
```

In the following lines, geometry parameters and the mesh size are defined. Regarding the geometry, the diameter and the length of the nanowire can be changed according to the specific simulation, while the radius r is calculated from the diameter.

```
### GEOMETRY: set here diameter and length ###################################

set d 40e-9; #diameter [m]
set r [expr {$d/2.}];
set l 1000e-9; #lenght [m]

### MESH SIZE: set here the dimension of each cell (cell_s) ################

set cell_s 5e-9
```

In the following lines, the name of the output file is set. The diameter of the wire (in nm) and the version number will be included in the output file name.

```
### BASENAME is used to define the name of output_file ######################

set d_nano [expr {$d*1e9}];
set vers_n 6; #can be used to distinguish more (1, 2, 3, 4,..)
set basename [format "OUT_FM_NANOWIRE_d%01.0f_vers%01.0f" $d_nano $vers_n ]
```

The following part of the code is divided in blocks. The first block is a function that defines a circle in the xy plane of radius r.

```
### The following three blocks define: ######################################
#    - a circle in the xy plane or radius r
#    - the length of the cylindrical wire to be l
#    - the discretization of the wire into cubic cells ######################

proc Circle { x y z } {
    global r d cell_s
    set test_r [expr {$x*$x+$y*$y}]
    set r_q [expr {$r*$r}]
    if {$test_r>$r_q} {return 0}
    return 1
}
```

The following block is a specific block for OOMMF simulations, it defines the Geometric volume of space for the simulation [4]. In this case the space for the simulation is defined as in figure 3.1.1.

```
Specify Oxs_ScriptAtlas:atlas [subst {
  xrange {-$r $r}
  yrange {-$r $r}
  zrange {0 $l}
  regions { Wire }
  script Circle
  script_args rawpt
}]
```

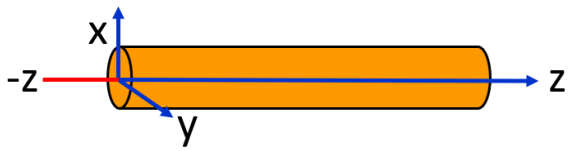

Figure 3.1.1 Schematic representation of the Geometric volume of space for the simulation (in orange)

The following block defines the rectangular mesh for the simulation.

```
Specify Oxs_RectangularMesh:mesh [subst {
  cellsize {$cell_s $cell_s $cell_s}
  atlas :atlas
}]
```

In the following lines of the code, the exchange energy, the magnetocrystalline energy, the demagnetizing energy and the Zeman energy are defined. It must be noticed that for the Zeman energy a spatially varying applied field is defined. The program will calculate the magnetization for each step of the applied field, allowing to simulate the hysteresis loop of the sample.

```
###########      ENERGIES      ##############################################

### EXCHANGE ENERGY ###########################################################

Specify Oxs_Exchange6Ngbr [subst {
  atlas :atlas
  A  {
    Wire Wire $A_Ni
  }
}]

### MAGNETOCRYSTALLINE ANISOTROPY: define here the easy axis ################

Specify Oxs_UniaxialAnisotropy [subst {
  K1  $K_Ni
  axis {0 0 1}
}]

### DEMAGNETIZING ENERGY ######################################################

Specify Oxs_Demag {}
```

```
### ZEEMAN ENERGY: specify here the external field ranges in [mT] ##########
# The change of external field is defined by each range as follows:
#     {    H_i_x  H_i_y  H_i_z   H_e_x  H_e_y  H_e_z    N_step }
#     where H_i_. H_e_. are cartesian components of the initial field
#     and the final field rispectively. N_step is the number of steps ######
Specify Oxs_UZeeman [subst {
  multiplier [expr {0.001/$mu0}]
  Hrange {
    {     0.01   0.01   0.01     0.01   0.01   1000     60 }
    {     0.01   0.01   0.01     0.01   0.01  -1000     60 }
  }
}]
```

Evolver and driver are also two specified blocks for OOMMF simulations. Evolvers are responsible for moving the simulation forward in individual steps and Drivers coordinate the action of the evolver on the whole simulation, by grouping steps into tasks, stages and runs [4].

```
###########     EVOLVER AND DRIVER    ####################################

### Energy Minimization Simulation: Conjugate Gradient Minimizer############
# The evolver updates the magnetization from one step to the next ##########

Specify Oxs_CGEvolve:evolve {}

### The driver coordinatse the action of the evolver on the simulation #####
# as a whole, by grouping steps into tasks, stages and runs.
# Define here the stopping criteria for a stage by choosing stopping_mxHxm #

Specify Oxs_MinDriver [subst {
 basename [list $basename]
 evolver :evolve
 stopping_mxHxm 0.1
 mesh :mesh
 Ms { Oxs_AtlasScalarField {
    atlas :atlas
    values {
       Wire $Ms_Ni
       universe 0.0
    }
 }}
```

```
m0 { Oxs_AtlasVectorField {
   atlas :atlas
   values {
      Wire {0 0 -1.0}
      universe {0 0 0}
   }
 }}
}]
```

3.2 Model for a core-shell system

To study the interaction with a possible external material that covers the surface of the nanowire, we modified and improved the Configuration file. Seeking to study only the interaction at the surface, it was possible to model a thin layer of the external material; this allowed to reduce the computational cost.

If a second magnetic material covers the ferromagnetic (FM) nanowire, at the interface a new exchange interaction keeps the magnetic moments of the FM core parallel to the magnetic moments of the shell. To explore this phenomenon, an external shell made by one layer of cells and with fixed magnetization was implemented in the configuration file. The magnetization of the core (which is free to move to reach the configuration of minimum energy) changes according to the external magnetic field and it is also influenced by the fixed magnetic moments of the shell. This coupling is called exchange bias effect and results in a shift of the hysteresis loop (see paragraph *2.5 Exchange bias effect*).

In the following pictures it is reported the code of the configuration file for the core-shell system. In the chapter *6. Appendix Tcl code files,* this code is reported as a text.

In the following lines of the code, two constants for later use and materials parameter are defined: the magnetization saturation, the exchange constant and the anisotropy constant of nickel and cobalt are defined and will be used for the core. To model an antiferromagnetic shell, a magnetization saturation equal to 0 is defined. This is because an antiparallel alignment of magnetic moments leads to a net magnetization which is 0. The exchange constant for the interface is also defined.

```
# MIF 2.1
# DESCRIPTION: Hysteresis loop of a cylindrical nanowire ###################
# Two materials are used, a core material and a shell material #############
# In this file is possible to change some parameters     ###################
# to understand their influence on the hysteresis loop   ###################
########## CONTANTS ############################################################

set pi [expr {4*atan(1.0)}]
set mu0 [expr {4*$pi*1e-7}]; #[N/A^2]

### MATERIAL PARAMETERS: default value of Co and Ni for OOMMF ##############

set Ms_Co 1400e3; #saturation magnetization [A/m]
set A_Co 30e-12; # exchange constant [J/m]
set K_Co 520e3; # anisotropy constant [J/m^3]
### ANTIFERROMAGNETIC SHELL MODEL ##############################################
set Ms_shell 0.01; #saturation magnetization [A/m]

### COUPLING INTERFACE: set the value of exchange constant at interface ####
set A_eb 7e-12;   #A[J/m]
```

In this second configuration file, geometry parameters and the mesh size are defined in the same way as in chapter 3.1.

In the following lines, the name of the output file is set. In this case, together with the diameter of the wire (in nm) and the version number, the exchange interaction at the interface is also included in the output file name.

```
### BASENAME is used to define the name of output_file ######################

set d_nano     [expr {$d*1e9}];
set A_eb_pico [expr {$A_eb*1e12}]; # exchange constant [pJ/m];
set vers_n 6; #can be used to distinguish more (1, 2, 3, 4,..)
set basename [format "OUT_FM+SHELL_NANOWIRE_d%01.0f_vers%01.0f" \
    $d_nano $vers_n]
```

The following part of the code is divided in blocks. The first block is a function that defines two concentric circles in the xy plane, one of radius r, one of radius $(r - cell\ size)$.

```
### The following three blocks define: #####################################
#    - a circle in the xy plane or radius r. Made by a core and a 5 nm shell
#    - the length of the cylindrical wire to be l
#    - the discretization of the wire into cubic cells ######################

proc Circle { x y z } {
    global r d cell_s
    set test_r [expr {$x*$x+$y*$y}]
    set r_q [expr {$r*$r}]
    set sl [expr {($r-$cell_s)*($r-$cell_s)}]
    if {$test_r<$r_q && $test_r>$sl } {return 2}
    if {$test_r<$sl } {return 1}
    return 0
}
```

The following block is a specific block for OOMMF simulations, it defines the Geometric volume of space for the simulation, named Atlas [4]. In this case the atlas is defined as in figure 3.2.1.

```
Specify Oxs_ScriptAtlas:atlas [subst {
  xrange {-$r $r}
  yrange {-$r $r}
  zrange {0 $l}
  regions { Wire W_shell}
  script Circle
  script_args rawpt
}]
```

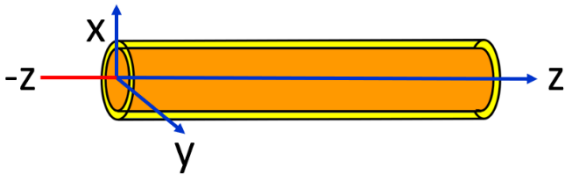

Figure 3.2.1 Schematic representation of the Geometric volume of space for the simulation, the core is represented in orange, the shell in yellow.

The specific OOMMF block for the definition of the rectangular mesh is identical to the in chapter 3.1.

In the following lines of the code, the exchange energy is defined. It must be noticed that this energy term is defined through the exchange constant. Only the interactions wire-wire and wire-shell are defined because the magnetic vectors of the shell are fixed.

```
############      ENERGIES      ##############################################

### EXCHANGE ENERGY ###########################################################

Specify Oxs_Exchange6Ngbr [subst {
  atlas :atlas
  A  {
    Wire Wire $A_Co
    Wire W_shell $A_eb
  }
}]
```

In the following lines the magnetocrystalline anisotropy is defined. This energy term will affect only the core of the system as the magnetic vectors of the shell are fixed.

```
### MAGNETOCRYSTALLINE ANISOTROPY: define here the easy axis ################

Specify Oxs_UniaxialAnisotropy [subst {
  K1  $K_Co
  axis {0 0 1}
}]
```

As the other energy terms the demagnetizing energy is defined by a specific OOMMF block. No specific parameters are required for its definition.

```
94  ### DEMAGNETIZING ENERGY ###############################################
95
96  Specify Oxs_Demag {}
```

The two following blocks are Evolver and Driver, two specific blocks for OOMMF simulations described in paragraph 3.1. In this case, in the evolver it is specified that the spins of the shell are fixed and not allowed to move according to the external magnetic field. While in the driver it is defined their orientation.

```
112 ###########     EVOLVER AND DRIVER    ######################################
113
114 ### Energy Minimization Simulation: Conjugate Gradient Minimizer############
115 # The evolver updates the magnetization from one step to the next ##########
116 # For the shell magnetization is fixed ####################################
117
118 Specify Oxs_CGEvolve:evolve { fixed_spins {  atlas  W_shell  }}
119
120 ### The driver coordinatse the action of the evolver on the simulation #####
121 # as a whole, by grouping steps into tasks, stages and runs.
122 # Define here the stopping criteria for a stage by choosing stopping_mxHxm #
123
124 Specify Oxs_MinDriver [subst {
125  basename [list $basename]
126  evolver :evolve
127  stopping_mxHxm 0.1
128  mesh :mesh
129  Ms { Oxs_AtlasScalarField {
130     atlas :atlas
131     default_value 0.0
132     values {
133        Wire $Ms_Co
134        W_shell $Ms_shell
135        universe 0.0
136     }
137  }}
138  m0 { Oxs_AtlasVectorField {
139     atlas :atlas
140     values {
141        Wire    {0 0  1.0}
142        W_shell {0 0 -1.0}
143        universe {0 0 0}
144     }
145  }}
146 }]
```

4. Simulation results: how geometry, material parameters and simulation conditions influence the magnetic response

The model permits to simulate the magnetic response of a ferromagnetic nanowire and to study its interaction with the surrounding material. The simulations presented in this chapter have been run with the aim to explore how the wire geometry and materials influence the magnetic response and the local magnetic moment distribution.

With the developed code it was possible to perform simulations on FM nanowires. Nanowires of two different materials and with different geometry were modelled to analyze their magnetic response. In particular, a nickel nanowire was used for the first simulations, and a cobalt nanowire was used for the other simulations. The materials parameters that have been used for these two materials are the ones presented in the chapter *2.2 Materials parameters*. For all the simulations, the nanowires length has been kept constant to 1 µm, while different diameters were used (40 nm, 60 nm or 80 nm).

The configuration file allows to define the magnetocrystalline easy axis, which can deviate from the applied field $\boldsymbol{H}$ with an angle β. This angle, in different simulations, has been set to 0°, 45°or 90°. Figure 4.1 shows a scheme of the wire and its system of coordinates; during all the performed simulations, the external field was applied along the z-axis, that corresponds to the wire axis.

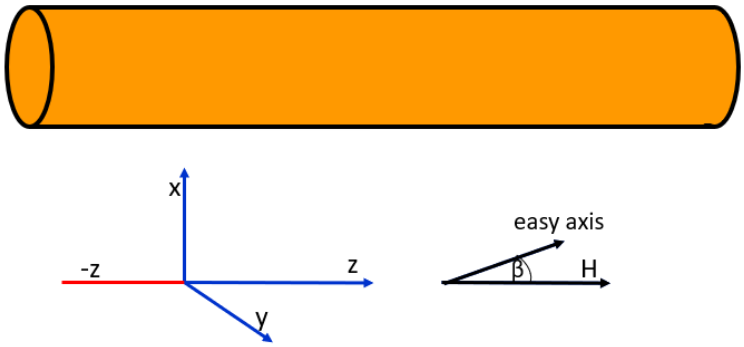

Figure 4.1 Sketch of the simulation model. The applied field is parallel to the z -axis.

The finite difference method used by OOMMF for the calculations divides the sample into a rectangular based mesh. The dimension of the cells is a parameter that must be specified in the model. To set this parameter two aspects should be considered. Firstly, the error associated with the staircase discretization of a curved object. Secondly, for a ferromagnetic sample, the cell size should not be bigger than the exchange length l_{ex} (see paragraph *2.7 Computational Micromagnetics in OOMMF*). During this study, most of the simulations were performed with a cubic mesh of length 5 nm, which is the same value of the exchange length of Co. Two simulations were also performed with a cubic mesh of length 2.5 nm.

For all the simulations, the method used to find the equilibrium state was the **Conjugate Gradient Minimizer**, that is an energy minimization method where the evolution to an energy minimum occurs through a sequence of line minimizations $[4]$. The system was considered to be at the equilibrium when the difference between reduced magnetization ($\boldsymbol{m} = \boldsymbol{M}/M_S$) and effective filed $\boldsymbol{H}$ was smaller than a tolerance value of 0.1 A/m.

Wire magnetic microstructure during Reversal Process

It is important to underline that micromagnetic simulations with the program OOMMF are not atomic simulations. To describe the magnetization configuration, the software calculates the vector field $\boldsymbol{M}$, a continuous function that represents the local average density of magnetic moments $\boldsymbol{\mu}_i$. To resolve $\boldsymbol{M}$, the software uses a Finite difference method which divides the sample into cells; each cell is considered to be homogeneously magnetized.

With the program it is possible to display and save the magnetization distribution along the sample. By observing the magnetization configuration during the **reversal process**, it is possible to identify the magnetization reversal mode that occurs.

In figure 4.1.1 it is possible to follow the reversal process of a nanowire of Co; the same section of the wire is shown during different steps of the reversal process, and the orientation of magnetization for each cell is represented by an arrow. By looking at the

different steps of the process, it is possible to see that a domain wall moves from the left surface to the center of the wire.

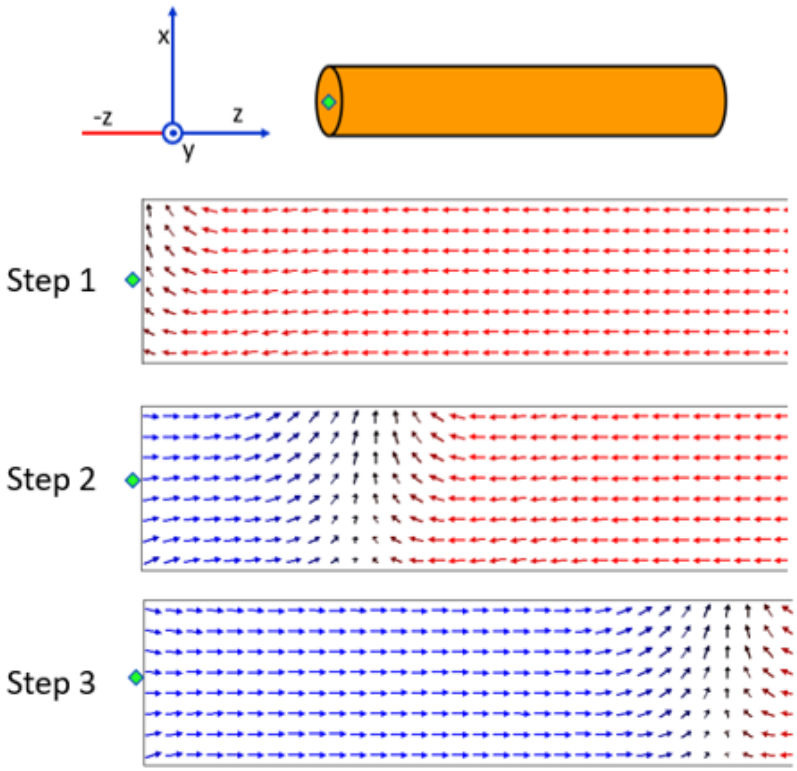

Figure 4.1.1. The magnetization along the wire has been simulated during different steps of the reversal process. A section of the Co wire along a plane perpendicular to y-axis is reported during different steps of the magnetization reversal process. Along each section, is displayed the magnetization orientation for each cell. The green rhombus is used to indicate the position of the cylinder base.

To better identify the type of domain wall it is also necessary to observe a section of the wire along a plane perpendicular to z-axis, as shown in figure 4.1.2. In this case, by observing the magnetization vector along different sections of the wire, it is possible to recognize that a transverse domain wall is present along the sample.

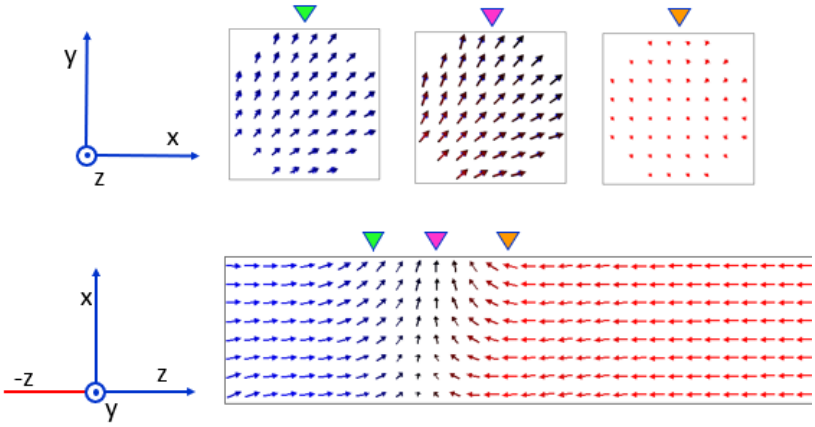

Figure 4.1.2 different wire sections are reported to show the transverse domain wall that is present along the wire. The triangular symbols are used to indicate the location of the circular section of the wire

4.1 Influence of diameter on the hysteresis loop

By performing three simulations on a Ni nanowire of different diameters, it was possible to explore how the hysteresis loop and the reversal mechanism change as a function of the aspect ratio.

The simulations have been performed on nanowires of the following diameters:

Table 4.1.1

Simulation	**diameter**
A	40 nm
B	60 nm
C	80 nm

The first outputs that can be analyzed are the hysteresis loop and the value of reversal field. In figure 4.1.1 the results for simulation A, B and C are presented. The smaller the aspect ratio (for bigger diameters) the smaller the value of reversal field. For a diameter of 80 nm the shape of the hysteresis loop is not squared.

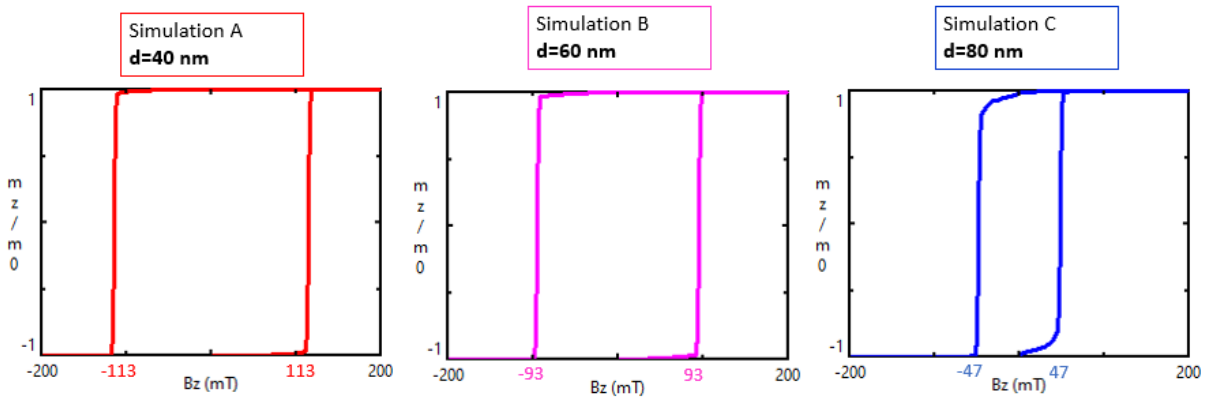

Figure 4.1.1 Hysteresis loops of simulations A, B and C.

4.1.1 Magnetization reversal process

As it is shown in figure 4.1.1.1, depending on their diameters, the magnetization of Ni nanowires reverses either with transverse domain wall or with vortex domain wall. For a diameter of 40 nm (simulation A) the domain wall is transverse type. When the Ni wire has a diameter of either 60 nm or 80 nm (simulation B and C) the reversal process occurs through the nucleation of a vortex. When the diameter is 80 nm the vortex structure is present along the whole nanowire length.

This result was compared to literature experimental studies. In particular, in the study [16] similar results have been obtained. For wires with a diameter smaller than 40 nm, a transverse domain wall nucleates and propagates along the nanowire axis, while the reversal of thick nanowires (diameter more than 40 nm) is achieved via localized curling or vortex mode.

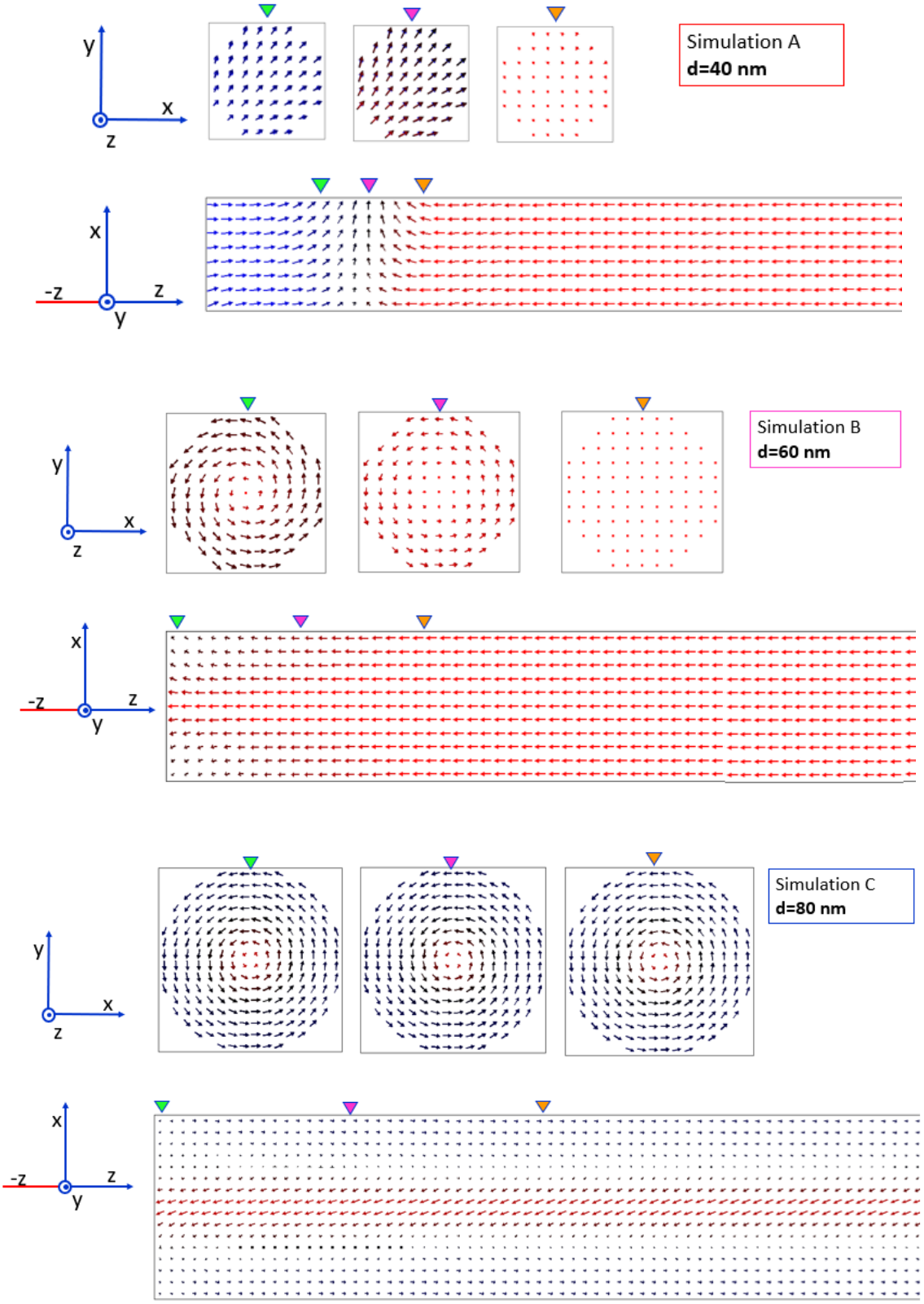

Figure 4.1.1.1 Sections of the wire for simulations A, B and C. The magnetic moments orientation for each cell is represented by arrows. The triangular symbols are used to indicate the position or the circular section along the wire.

4.2 Effects of easy-axis deviations from the applied field

The easy axis for the magnetization can deviate with respect to the wire axis (z-axis in the wire system of coordinates) by an angle β. By performing three simulations on a Co wire it was possible to explore its influence on the magnetic response of the sample, and study how the hysteresis loop changes as a function of the magnetocrystalline anisotropy direction.

The external applied field was always aligned along z-axis, and the angle β was set as follows:

Table 4.2.1

Simulation	**Angle β**
D	0°
E	45°
F	90°

Figure 4.2.1 shows the hysteresis loops for the three simulations. In table 4.2.2 the values of reversal field and remanence are reported. Comparing the results, it is possible to observe that the reversal field and the remanence strongly decrease as β increases. When β=0° the hysteresis loop is squared. While for β=90° no remanence and coercivity are observed.

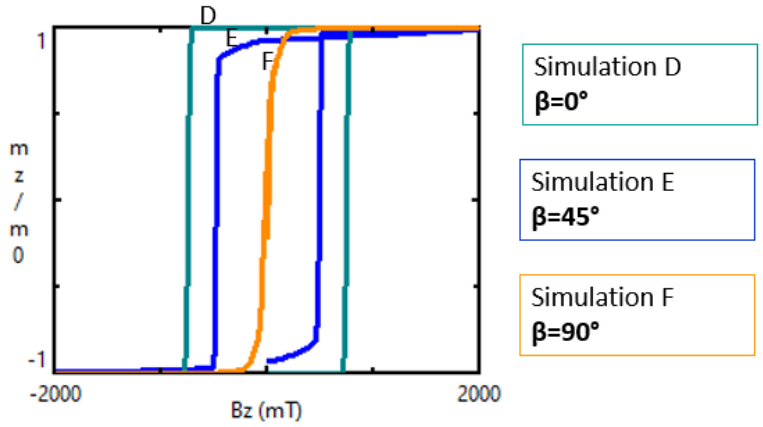

Figure 4.2.1 hysteresis loops of simulations D, E and F.

Table 4.2.2

Simulation	**Angle β**	**Reversal field H_{rev}**	**Remanence m_z/m_0**
D	0°	730 mT	1
E	45°	470 mT	0.93
F	90°	0 mT	0

Similar results have been obtained in literature. In the study [3], the authors investigate the influence of the deviation of easy axis on the coercivity and magnetization reversal process via 3D micromagnetic simulations. The study proves that the coercivity and remanence decrease linearly with as the easy axis deviation grows.

4.3 Effects of cell size reduction

As mentioned in the paragraph *Material parameters*, the **exchange length** (l_{ex}) is the property that governs the width of a domain wall. To perform a simulation on a ferromagnetic object, the cell size should not be bigger than the exchange length**.**

For the last performed simulations on a Co nanowire, the cell size was set at the same value of the exchange length (5 nm).

A second consideration should be done. During the simulation, the wire is divided into cubic cells of 5nm length and the results are limited by the mesh resolution. It might have occurred that for small wires this mesh resolution was not good enough to simulate the magnetic response of the sample properly.

By performing a simulation with a smaller cell size on a Co wire of diameter 40 nm, it was possible to verify that the magnetic response and the reversal mechanism have been calculated correctly.

For the new simulation (simulation D.2) the geometry and all the material parameters have been set as in simulation D. The only difference is the cell size, that has been defined as follows:

Table 4.3.1

Simulation	**Cell size**
D	5 nm
D.2	2,5 nm

The first result that is possible to compare is the hysteresis loop. In figure 4.3.1 it is possible to observe that the two loops overlap.

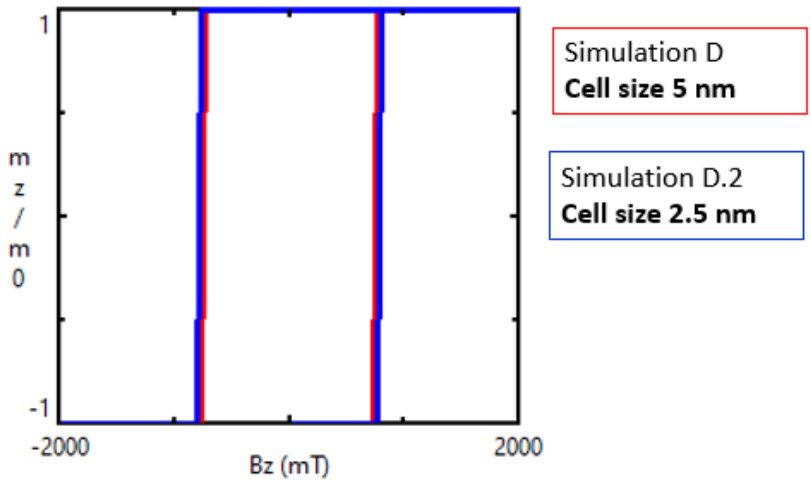

Figure 4.3.1 Hysteresis loops of simulations D and D.2

4.3.1 Magnetization reversal process

As it is shown in figure 4.3.1.1, the reverse of the magnetization happens through the nucleation and propagation of a transverse domain wall in both simulations. By comparing the magnetic configuration of the two simulations, it is possible to see that the domain wall occupies the same width along the wires, but it can be defined with more accuracy when the cell size is smaller.

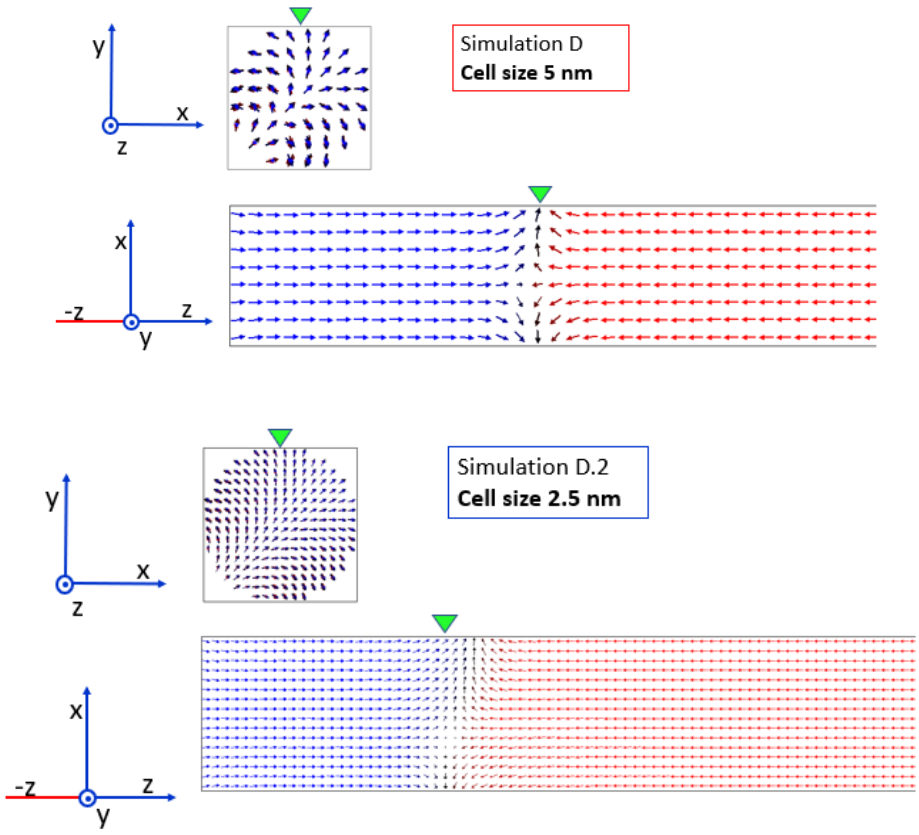

Figure 4.3.1.1 Sections of the wire for simulation D and D.2. The magnetic moments orientation for each cell is represented by arrows. The triangular symbols are used to indicate the position or the circular section along the wire.

4.4 Exchange bias effect

The exchange bias phenomenon is a surface effect that can happen when the magnetic moments of the wire are influenced by the surrounding material, for example if an antiferromagnetic shell covers the surface wire. The coupling between the magnetic moments of the wire and the shell results in a displacement of the hysteresis loop.

To explore the phenomenon of exchange bias, an external shell made by one layer of cells and with fixed magnetization was implemented in the configuration file. By modifying the exchange interaction at the interface, it is possible to simulate the coupling core-shell.

To simulate an antiferromagnetic material in computational micromagnetics is difficult because the FDM does not allow to model the magnetic moments of the single atoms, it

only calculates the overall magnetization resulting in each single cell. Therefore, the only possible way to model an antiferromagnetic material is to set the overall magnetization saturation to zero. This fact holds also for real AFM samples where the antiparallel magnetic moments compensate and result in a total magnetization that is close to 0. It must be noticed that in the LLG equation (equation 2.6.5.4) the evolution of magnetization is proportional to $1/M_S$. This equation is used by the program to calculate the magnetization configuration, therefore a value different from exact 0 should be assigned to M_S. Considering these aspects, for the simulations of exchange bias between a FM core and an AFM shell, the magnetization saturation of the shell has been set as follows:

$$M_{S\_shell}=0.01 \text{ A/m}$$

Figure 4.4.1 shows the magnetization along the wire in this new configuration during different moments of the reversal mechanism. The empty arrows show the direction of the fixed spins of the shell.

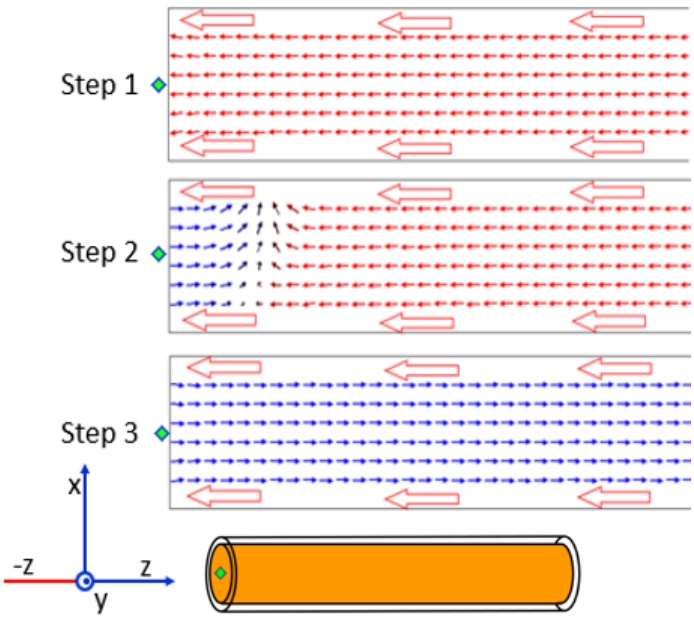

Figure 4.4.1 Magnetic moments distribution along a section of the core-shell wire during different steps of the reversal process. The green rhombus is used to indicate the position of the cylinder base.

By performing a first simulation with the improved model it was possible to verify that a coupling at the interface results in a shift of the hysteresis loop. Simulation G was performed

on a Co wire of diameter 40 nm, the value of 7 pJ/m was used as exchange constant at the interface.

This first reference value was established by a research in literature. In the study [9] the authors performed a micromagnetic simulation on a thin film made of Co/CoO. The value of exchange constant used at the interface in this study was A_{pin} = 6.9×10^{-12} J /m. With this value the authors were able to reproduce experimental data for a polycrystalline Co/CoO bilayer.

In figure 4.4.2 it is shown the corresponding hysteresis loop. Starting from a negative magnetization (point 1 in figure), in order to switch to positive magnetization, an external field of 1130 mT is needed. On the contrary, starting from a positive magnetization (point 3 in figure), to switch to negative magnetization, an external field of is 600 mT is needed. This shift of the hysteresis loop is due to the coupling with the shell: starting parallel to the shell, the magnetic moments of the core are in a stable position, and a big external field is needed to change configuration to antiparallel to the shell; once antiparallel, a smaller field is necessary to switch to the parallel configuration.

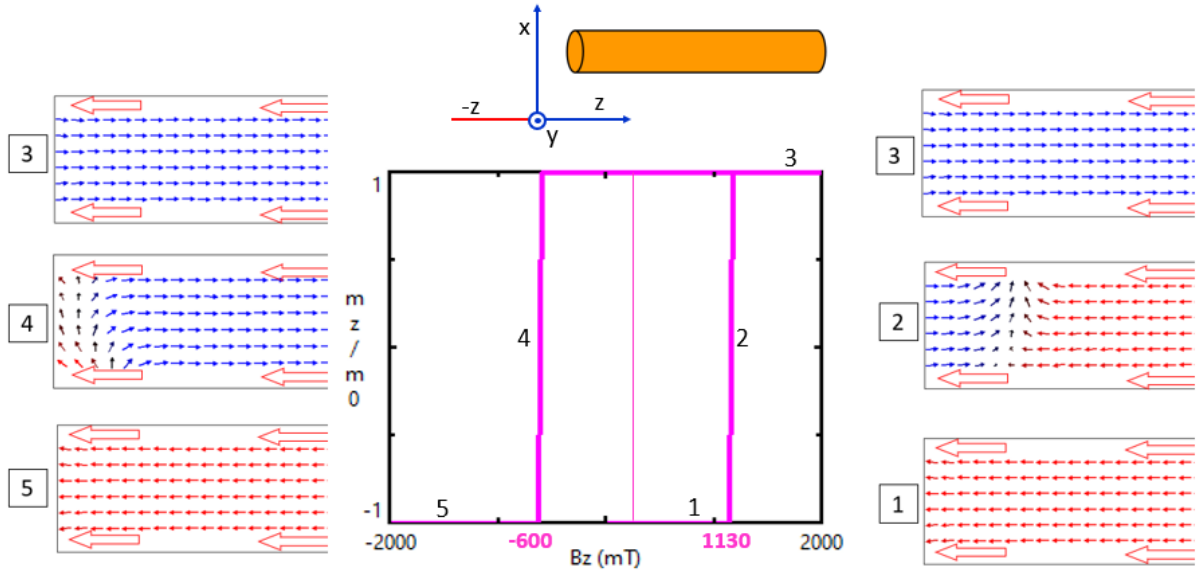

Figure 4.4.2 Hysteresis loop and a section of the wire during different steps of the hysteresis loop for simulation G. Numbers on the loop are used to identify steps of the hysteresis loop. For each step it is shown the magnetization configuration of the wire (diameter 40 nm). The magnetic moments orientation for each cell is represented by arrows.

4.5 Influence of the exchange interaction on the displacement of the loop

By performing some simulations with a different value of exchange constant at the interface, it was possible to prove that the displacement is controlled by the exchange interaction at the surface.

The simulations have been performed by changing only the value of exchange constant at the interface core-shell. The values were set as follows:

Table 4.5.1

Simulation	**Exchange constant A_{eb}**
G	7 pJ/m
H	3 pJ/m
I	0,03 pJ/m

In figure 4.5.1 the hysteresis loop of simulations F, G and H are compared and in table 4.5.2 the values of the reversal field (in mT) are compared. With a weak coupling at the interface the hysteresis loop is symmetric, and when the coupling increases the displacement of the loop increases.

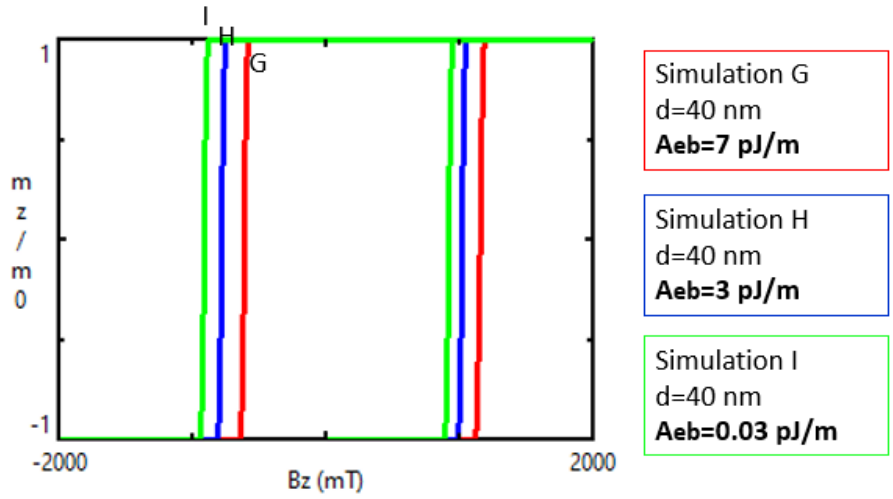

Figure 4.5.1 Hysteresis loops of simulations G, H and I.

Table 4.5.2

Simulation	**Exchange constant A_{eb}**	**$\lvert H_{rev} \rvert$ left**	**$\lvert H_{rev} \rvert$ right**
G	7 pJ/m	600 mT	1130 mT
H	3 pJ/m	760 mT	1000 mT
I	0,03 pJ/m	900 mT	900 mT

4.6 Influence of wire diameter on the displacement of the loop

By performing other simulations on Co wires of different diameters and an antiferromagnetic shell, it was possible to prove that the exchange bias is a surface effect and its efficacy depends on the ratio interface/volume. If the diameter increases, the ratio interface/volume decreases, and the displacement of the loop gets smaller.

The simulations have been performed by changing the diameter of the wire, while the thickness of the non-magnetic shell was kept constant to 5 nm. The values for the total diameter (of the system core and shell) have been set as follows:

Table 4.6.1

Simulation	**diameter**
G	40 nm
L	60 nm
M	80 nm

The hysteresis loop for simulation G L and M are shown in figure 4.6.1, and table 4.6.2 reports the values of the reversal field for the left and right side of the loop and the discrepancy between the two values. It is possible to notice that the bigger the diameter the smaller the displacement of the hysteresis loop and the discrepancy between the two values of reversal field.

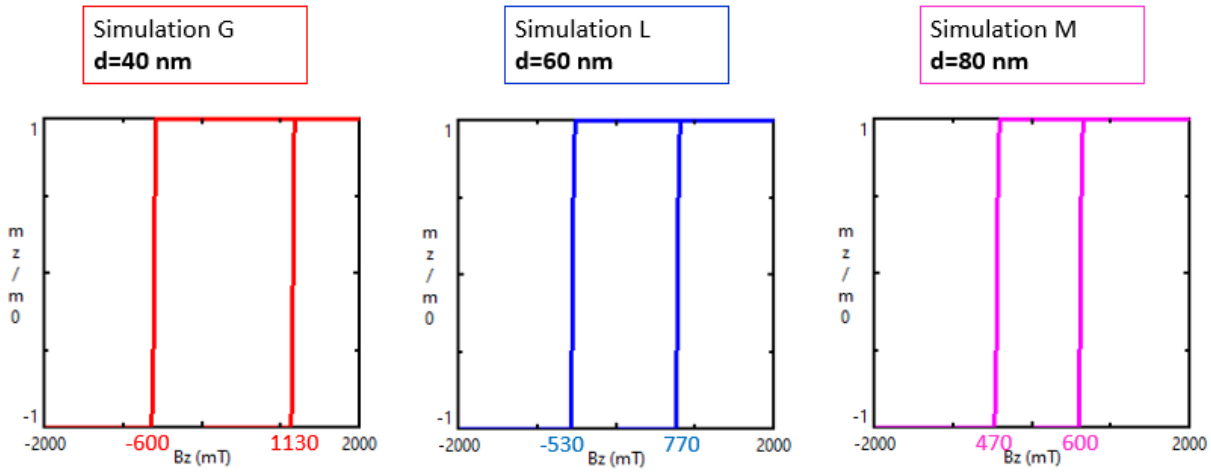

Figure 4.6.1 Hysteresis loops of simulations G, L and M

Table 4.6.2

Simulation	**|Hrev | left**	**|Hrev | right**	**|Hrev|right - |Hrev|left**
G	600 mT	1130 mT	533 mT
L	530 mT	770 mT	240 mT
M	470 mT	600 mT	130 mT

4.7 Influence of a shell stray field on the displacement of the loop

As mentioned, in an antiferromagnetic material, the magnetic moments are antiparallel and compensate each other resulting in a negligible external stray field.

It is important to mention that this is not true in ferromagnetic shells where the magnetic moments are parallel. Therefor the external stray field in this case is not negligible and it affects the final results.

To see this fact, a simulation using a sample made of a ferromagnetic core and a ferromagnetic shell was performed and compared with the previous case. The values of saturation magnetization of the shell for the two simulations are presented in the following table:

Table 4.7.1

Simulation	**Magnetic saturation**
G	M_{S_shell}=0.01 A/m
N	M_{S_shell}=1400 A/m

The first outputs that it is possible to analyze are the hysteresis loop and its displacement. In figure 4.7.1 the results for simulation G and N are presented. In both cases the shell is modelled as made of fixed magnetic moments, but when the magnetic saturation of the shell is the typical order of magnitude of ferromagnetic materials, the displacement of the loop is 100 mT smaller.

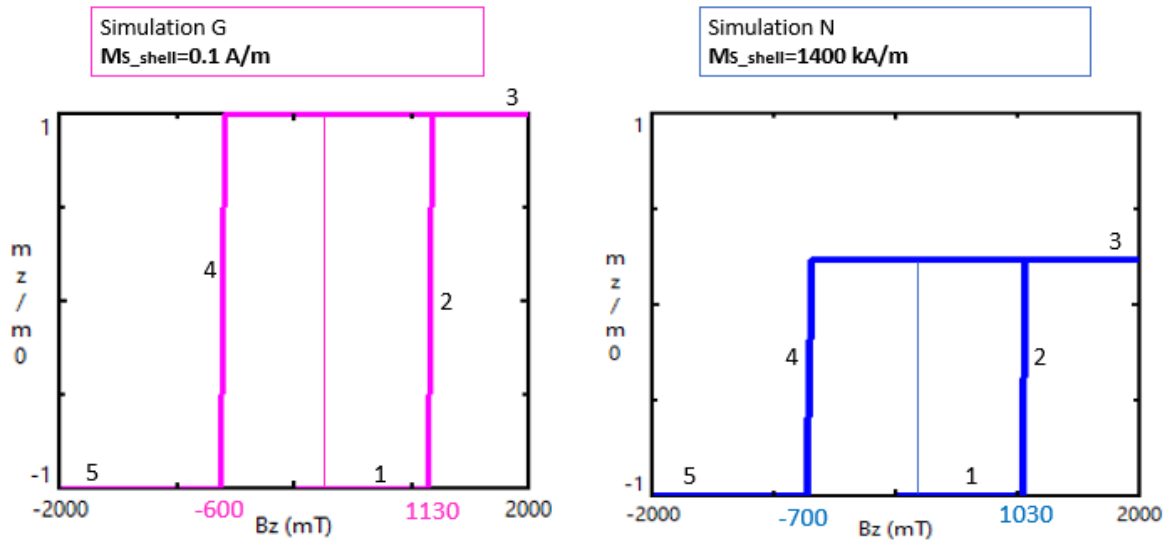

Figure 4.7.1 Hysteresis loops of simulations G and N. For simulation N the relative magnetization along z (m_z/m_0) never reaches the value 1 because of the magnetic moments of the shell.

With some energy considerations it was possible to further analyze the effect of the stray field going out from a ferromagnetic shell. As a second consideration, by comparing the thermal energy and the demagnetizing energy, it was possible to see that the room temperature is a low temperature for the system.

4.7.1 Energy considerations

For every point of the hysteresis loop, the program provides the value for all the energy terms. Table 4.7.1.1 reports the values of the demagnetizing energy (demag energy) at positive and negative saturation (point 3 and 5 of the hysteresis loops in figure 4.7.1) for simulations G and N. For simulation G the demagnetizing energy is identical for positive and negative saturations and this is because the stray field is negligible and it doesn't affect the results. On the contrary, for simulation N the demagnetizing energies are different at positive and negative saturations because in the first case (3) part of the magnetization field of the core is compensated by **the stray field of the shell** resulting in a small total energy, while in the second case (5) the magnetization field and the stray field of the shell sum up leading to a bigger total energy.

Table 4.7.1.1

Simulation	**Magnetic saturation shell**	**Saturation point**	**Demag energy**
G	M_{S_shell}=0.01 A/m	Positive saturation (3)	$E_{demag} = 0{,}013$ fJ
G	M_{S_shell}=0.01 A/m	Negative saturation (5)	$E_{demag} = 0{,}013$ fJ
N	M_{S_shell}=1400 A/m	Positive saturation (3)	$E_{demag} = 0{,}007$ fJ
N	M_{S_shell}=1400 A/m	Negative saturation (5)	$E_{demag} = 0{,}027$ fJ

Finally, the demagnetization energy can be compared with the thermal energy. At room temperature, the thermal energy of a system is:

Equation 4.7.1.1

$$K_B T = 25\ meV$$

By converting the demagnetizing energy in eV, it was possible to observe that room temperature can be considered a low temperature for the system:

Equation 4.7.1.2

$$1eV = 1{,}6 * 10^{-19} J$$

Equation 4.7.1.3

$$0{,}013\ (fJ) = 13 * 10^{-18}(J) = \frac{13 * 10^{-18}(J)}{1{,}6 * 10^{-19}\left(\frac{J}{eV}\right)} = 81,25\ (eV)$$

$$E_{Demag} = 81{,}25\ eV$$

$$K_B T = 0{,}025 eV$$

By comparing $K_B T$ and E_{Demag} it can be seen that, at room temperature, the thermal energy of the system is three order of magnitude smaller than the demagnetizing energy. The other energy terms of the magnetic energy equation are of the order of $10^{-15}\ J$ as the demagnetizing energy, thus this consideration is valid for the total energy of the system.

5. Conclusion: a summary of the considered aspects

To summarize this work, in the introduction we saw that Ferromagnetic nanowires are promising candidates for several applications, for example magnetic memories, and that the characterization of the magnetic texture is important for the development of magnetic devices.

Micromagnetic simulations are a powerful tool that permits to characterize the magnetization reversal process of ferromagnetic nanowires.

For this study we made use of the Micromagnetic Simulation **program OOMMF**. The software uses a **finite difference (FD) method** for the discretization of the sample and divides the sample into equal sized cells.

The input for the program is a **configuration file**, a text file written in the Tcl syntax, that will be read by the simulation tool at run time to define the sample geometry, the materials that characterize the sample, and all the simulation conditions.

The **aim** of this work was to develop a configuration file to simulate the magnetic response of a ferromagnetic nanowire and perform some simulations to explore how the magnetic response (Hysteresis loop and Magnetic texture) is influenced by wire geometry, by materials parameters and by the interaction with the surrounding material. The developed Model was designed to simulate a magnetic nanowire in one of the following configurations:

- made of a FM material
- made by a FM core and an AFM shell

By performing several simulations, it was possible to investigate the influence of geometry and material parameters on the macroscopic magnetic response and on the magnetic moments distribution along the sample.

The first parameter investigated was the **aspect ratio**. The length of the wire was kept constant while different diameters have been used to run three simulations on Ni wires. For smaller aspect ratios the hysteresis loop results less squared, and the reversal mechanism starts at smaller values of external field. It was possible to observe that, depending on the diameters, the magnetization of a nanowire can reverse with transverse domain wall or vortex domain wall. For a nickel nanowire with a diameter of 40 nm the domain wall is transverse type, while for bigger diameters the domain wall is vortex type.

The **magnetocrystalline anisotropy** was the second parameter analyzed. The influence of easy-axis deviation from the direction of the applied field was investigated on a cobalt nanowire. For this system, the reversal field and the remanence strongly decrease with the increment of the deviation angle.

Simulations with different cell size have been performed on a Co wire of diameter 40 nm to explore the influence of cell size reduction on the magnetic response. It was possible to see that the domain wall occupies the same width along the wires, but it is defined with more accuracy when the cell size is smaller.

The model successfully simulated the coupling of magnetic moments at the interface between a ferromagnetic material and an antiferromagnetic shell, resulting in a displacement of the hysteresis loop.

By performing some simulations with different values of exchange constant, it was possible to verify that the shift of the hysteresis loop is controlled by the exchange interaction. By performing some simulations with different diameters of the wire, it was possible to understand that the **exchange bias** is a surface effect, and its relevance depends on the ratio surface/volume. The smaller the ratio the stronger the effect.

The code was designed to model only one layer of external shell. According to the nature and the material of the shell, the total demagnetizing field can be negligible (for antiferromagnetic shells) or it can influence the displament of the loop (for ferromagnetic shells). If the shell is modelled as antiferromagnetic (the magnetization saturation M_S of the

shell is set to a value close to 0), then there is no influence of the shell on the demagnetizing field. On the contrary, when the shell is modelled as one layer of ferromagnetic material, the stray field of the shell influences the total demagnetizing field and the resulting hysteresis loop is different.

Finally, it is worth mentioning that the magnetic response (the reversal field and the magnetization reversal process) of an array of nanowires depend not only on the magnetic properties of each nanowire, but also on the interaction between close nanowires [2, 11].

The model created during this work for the simulation of a ferromagnetic wire with exchange bias can be expanded to study the interaction between ferromagnetic nanowires in an array, and this was the topic of another project in which I took part during my exchange as an Erasmus student.

6. Appendix Tcl code file

6.1 Tcl configuration file for simple cylindrical nanowire

```
########## CONTANTS ##########################################################

set pi [expr {4*atan(1.0)}]
set mu0 [expr {4*$pi*1e-7}]; #[N/A^2]

### MATERIAL PARAMETERS: default value of Co and Ni for OOMMF ##############

set Ms_Co 1400e3; #saturation magnetization [A/m]
set A_Co 30e-12; # exchange constant [J/m]
set K_Co 520e3; # anisotropy constant [J/m^3]

set Ms_Ni 490e3; #saturation magnetization [A/m]
set A_Ni 9e-12; # exchange constant [J/m]
set K_Ni -5.7e3; # anisotropy constant [J/m^3]


### GEOMETRY: set here diameter and length ###################################

set d 40e-9; #diameter [m]
set r 20e-9;
set l 1000e-9; #lenght [m]

### MESH SIZE: set here the dimension of each cell (cell_s) ################

set cell_s 5e-9


### BASENAME is used to define the name of output_file #####################

set d_nano [expr {$d*1e9}];
set vers_n 6; #can be used to distinguish more (1, 2, 3, 4,..)
set basename [format "OUT_FM_NANOWIRE_d%01.0f_vers%01.0f" $d_nano $vers_n ]


### The following three blocks define: ######################################
#   - a circle in the xy plane or radius r
#   - the length of the cylindrical wire to be l
#   - the discretization of the wire into cubic cells ######################

proc Circle { x y z } {
    global r d cell_s
       set test_r [expr {$x*$x+$y*$y}]
       set r_q [expr {$r*$r}]
    if {$test_r>$r_q} {return 0}
    return 1
}

Specify Oxs_ScriptAtlas:atlas [subst {
  xrange {-$r $r}
  yrange {-$r $r}
  zrange {0 $l}
  regions { Wire }
  script Circle
  script_args rawpt
}]

Specify Oxs_RectangularMesh:mesh [subst {
  cellsize {$cell_s $cell_s $cell_s}
  atlas :atlas
}]
```

```
############      ENERGIES      ##############################################

### EXCHANGE ENERGY ###########################################################

Specify Oxs_Exchange6Ngbr [subst {
  atlas :atlas
  A  {
    Wire Wire $A_Ni
  }
}]

### MAGNETOCRYSTALLINE ANISOTROPY: define here the easy axis ###############

Specify Oxs_UniaxialAnisotropy [subst {
  K1  $K_Ni
  axis {0 0 1}
}]

### DEMAGNETIZING ENERGY ######################################################

Specify Oxs_Demag {}

### ZEEMAN ENERGY: specify here the external field ranges in [mT] ###########
# The change of external field is defined by each range as follows:
#     {    H_i_x  H_i_y  H_i_z   H_e_x  H_e_y  H_e_z    N_step }
#     where H_i_. H_e_. are cartesian components of the initial field
#     and the final field rispectively. N_step is the number of steps ######

Specify Oxs_UZeeman [subst {
  multiplier [expr {0.001/$mu0}]
  Hrange {
      {     0.01   0.01   0.01     0.01   0.01   1000     60 }
      {     0.01   0.01   0.01     0.01   0.01  -1000     60 }
  }
}]

############     EVOLVER AND DRIVER    ######################################

### Energy Minimization Simulation: Conjugate Gradient Minimizer#############
# The evolver updates the magnetization from one step to the next ###########

Specify Oxs_CGEvolve:evolve {}

### The driver coordinates the action of the evolver on the simulation #####
# as a whole, by grouping steps into tasks, stages and runs.
# Define here the stopping criteria for a stage by choosing stopping_mxHxm #

Specify Oxs_MinDriver [subst {
 basename [list $basename]
 evolver :evolve
 stopping_mxHxm 0.1
 mesh :mesh
 Ms { Oxs_AtlasScalarField {
    atlas :atlas
    values {
       Wire $Ms_Ni
          universe 0.0
    }
 }}
 m0 { Oxs_AtlasVectorField {
    atlas :atlas
    values {
```

```
        Wire {0 0 -1.0}
             universe {0 0 0}   } }} }]
```

6.2 Tcl configuration file for a core-shell system

```
# MIF 2.1
# DESCRIPTION: Hysteresis loop of a cylindrical nanowire ###################
# Two materials are used, a core material and a shell material #############
# In this file is possible to change some parameters     ###################
# to understand their influence on the hysteresis loop   ###################

########## CONTANTS ##########################################################

set pi [expr {4*atan(1.0)}]
set mu0 [expr {4*$pi*1e-7}]; #[N/A^2]

### MATERIAL PARAMETERS: default value of Co and Ni for OOMMF ##############

set Ms_Co 1400e3; #saturation magnetization [A/m]
set A_Co 30e-12; # exchange constant [J/m]
set K_Co 520e3; # anisotropy constant [J/m^3]

set Ms_Ni 490e3; #saturation magnetization [A/m]
set A_Ni 9e-12; # exchange constant [J/m]
set K_Ni -5.7e3; # anisotropy constant [J/m^3]

### ANTIFERROMAGNETIC SHELL MODEL ############################################
set Ms_shell 0.01; #saturation magnetization [A/m]

### GEOMETRY: set here diameter and length ###################################

set d 40e-9; #diameter [m]
set r 20e-9;
set l 1000e-9; #lenght [m]

### MESH SIZE: set here the dimension of each cell (cell_s) #################

set cell_s 5e-9

### COUPLING INTERFACE: set the value of exchange constant at interface ####
set A_eb 7e-12;  #A[J/m]

### BASENAME is used to define the name of output_file ######################

set d_nano    [expr {$d*1e9}];
set A_eb_pico [expr {$A_eb*1e12}]; # exchange constant [pJ/m];
set vers_n 6; #can be used to distinguish more (1, 2, 3, 4,..)
set basename [format "OUT_FM+SHELL_NANOWIRE_d%01.0f_vers%01.0f" \
    $d_nano $vers_n]

### The following three blocks define: ######################################
#   - a circle in the xy plane or radius r. Made by a core and a 5 nm shell
#   - the length of the cylindrical wire to be l
#   - the discretization of the wire into cubic cells ######################

proc Circle { x y z } {
    global r d cell_s
       set test_r [expr {$x*$x+$y*$y}]
       set r_q [expr {$r*$r}]
```

```
      set sl [expr {($r-$cell_s)*($r-$cell_s)}]
    if {$test_r<$r_q && $test_r>$sl } {return 2}
      if {$test_r<$sl } {return 1}
      return 0
}

Specify Oxs_ScriptAtlas:atlas [subst {
  xrange {-$r $r}
  yrange {-$r $r}
  zrange {0 $l}
  regions { Wire W_shell}
  script Circle
  script_args rawpt
}]

Specify Oxs_RectangularMesh:mesh [subst {
  cellsize {$cell_s $cell_s $cell_s}
  atlas :atlas
}]


############      ENERGIES      ##############################################

### EXCHANGE ENERGY ###########################################################

Specify Oxs_Exchange6Ngbr [subst {
  atlas :atlas
  A  {
    Wire Wire $A_Co
      Wire W_shell $A_eb
  }
}]

### MAGNETOCRYSTALLINE ANISOTROPY: define here the easy axis ###############

Specify Oxs_UniaxialAnisotropy [subst {
  K1  $K_Co
  axis {0 0 1}
}]

### DEMAGNETIZING ENERGY ######################################################

Specify Oxs_Demag {}

### ZEEMAN ENERGY: specify here the external field ranges in [mT] ##########
# The change of external field is defined by each range as follows:
#     {    H_i_x  H_i_y  H_i_z   H_e_x  H_e_y  H_e_z    N_step }
#     where H_i_. H_e_. are cartesian components of the initial field
#     and the final field rispectively. N_step is the number of steps ######

Specify Oxs_UZeeman [subst {
  multiplier [expr {0.001/$mu0}]
  Hrange {
      {     0.01   0.01   0.01     0.01   0.01   2000     60 }
        {     0.01   0.01   0.01     0.01   0.01  -2000     60 }
  }
}]

############     EVOLVER AND DRIVER    ######################################

### Energy Minimization Simulation: Conjugate Gradient Minimizer#############
# The evolver updates the magnetization from one step to the next ##########
# For the shell magnetization is fixed ####################################
```

```
Specify Oxs_CGEvolve:evolve { fixed_spins {  atlas  W_shell  }}

### The driver coordinatse the action of the evolver on the simulation #####
# as a whole, by grouping steps into tasks, stages and runs.
# Define here the stopping criteria for a stage by choosing stopping_mxHxm #

Specify Oxs_MinDriver [subst {
 basename [list $basename]
 evolver :evolve
 stopping_mxHxm 0.1
 mesh :mesh
 Ms { Oxs_AtlasScalarField {
    atlas :atlas
       default_value 0.0
    values {
       Wire $Ms_Co
          W_shell $Ms_shell
          universe 0.0
    }
 }}
 m0 { Oxs_AtlasVectorField {
    atlas :atlas
    values {
         Wire    {0 0  1.0}
              W_shell {0 0 -1.0}
              universe {0 0 0}
    }
 }}
}]
```

7. Bibliography

[1] M. Beg, R. A. Pepper, and H. Fangohr. **2017**, User interfaces for computational science: A domain specific language for OOMMF embedded in Python. *AIP Advances,* vol 7, issue 56025.
DOI: 10.1063/1.4977225

[2] A. Kuncserab, S. Antoheb. V. Kuncser. **2017**, A general perspective on the magnetization reversal in cylindrical soft magnetic nanowires with dominant shape anisotropy. Journal of Magnetism and Magnetic Materials, vol. 423, pp. 34-38.
DOI: 10.1016/j.jmmm.2016.09.066

[3] Y. Peng, M. Yue, H. Li, Y. Li, C. Li, H. Xu, Q. Wu, W. Xi. **2018**, The Effect of Easy Axis Deviations on the Magnetization Reversal of Co Nanowire. *IEEE Transactions on Magnetics*, vol. 54, no. 11, pp. 1-5.
DOI: 10.1109/TMAG.2018.2831671.

[4] M. J. Donahue, D.G. Porter. **1999**, OOMMF User's Guide, Version 1.0. *National Institute of Standards and Technology, Gaithersburg, MD.* Interagency Report NISTIR 6376.
DOI: 10.6028/NIST.IR.6376; OOMMF home page: http://math.nist.gov/oommf

[5] S. S. P. Parkin, M. Hayashi and L. Thomas. **2008**, Magnetic domain-wall racetrack memory. *Science*, vol. 320, no. 5873, pp. 190-194.
DOI: 10.1126/science.1145799

[6] Sachin Krishnia. **2017**, Current-driven domain wall dynamics in coupled ferromagnetic structures. *Doctoral Thesis at Nanyang Technological University, School of Physical and Mathematical Sciences, Singapore.*

[7] W. Zhou, J. Um, Y. Zhang, A. P. Nelson, Z. Nemati, J. Modiano, B. Stadler, R. Franklin. **2019**, Development of a Biolabeling System Using Ferromagnetic Nanowires. *IEEE Journal Of Electromagnetics, RF, and Microwaves in Medicine And Biology*, vol. 3, no. 2, pp. 134-142.
DOI: 10.1109/JERM.2018.2889049.

[8] Serrà, E. Vallés, J. García-Torres. **2017**, Electrochemically synthesized nanostructures for the manipulation of cells: Biohybrid micromotors. *Electrochemistry Communications*, vol. 85, 2017, pp. 27–31. DOI: 10.1016/j.elecom.2017.11.002

[9] M. A. Frantiu. **2019**, Micromagnetic Simulations of Magnetic Thin Films using MuMax3. *Master Thesis at University of Groningen*

[10] R. P. Boardman. **2005**, Computer simulation studies of magnetic nanostructures. *Doctoral Thesis at University of Southampton, School of Engineering Sciences, Computational Engineering and Design Group, United Kingdom.*

[11] M. Proenca, J.L. Prieto, Universitad Politacnica de Madrid. Course Spintronics and Nanomagnetism, slides of the academic course, year 2020.

[12] G. Barrera, P. Tiberto, P. Allia, B. Bonelli, S. Esposito, A. Marocco, M. Pansini, Y. Leterrier. **2019**, Magnetic Properties of Nanocomposites. *Applied Science*, vol. 9, issue 2.
DOI: 10.3390/app9020212

[13] J. Cantu-Valle, I. Betancourt, J. E. Sanchez, F. Ruiz-Zepeda, M. M. Maqableh, F. Mendoza-Santoyo, B. J. H. Stadler, A. Ponce. **2015**, Mapping the magnetic and crystal structure in cobalt nanowires. *Journal of Applied Physics,* vol. 118, issue 2.

DOI: 10.1063/1.4923745

[14] G. S. Abo, Y. Hong, J. Park, J. Lee, W. Lee and B. Choi. **2013**, Definition of Magnetic Exchange Length. *IEEE Transactions on Magnetics*, vol. 49, no. 8, pp. 4937-4939.
DOI: 10.1109/TMAG.2013.2258028

[15] O. Albrecht, R. Zierold, S. Allende, J. Escrig, C. Patzig, B. Rauschenbach, K. Nielsch, D. Görlitz. **2011**, Experimental evidence for an angular dependent transition of magnetization reversal modes in magnetic nanotubes" Journal of Applied Physics 109, 093910
DOI: 10.1063/1.3583666

[16] K. Ounadjela, R. Ferré, L. Louail, J. M. George and J. L. Maurice, L. Piraux and S. Dubois. **1997**, Magnetization reversal in cobalt and nickel electrodeposited nanowires. Journal of Applied Physics, vol.81, issue 8.
DOI: 10.1063/1.364568

[17] R. Hertel. **2001**, Micromagnetic simulations of magnetostatically coupled Nickel nanowires. *Journal of Applied Physics,* vol. 90, issue 5.
DOI: 10.1063/1.1412275

[18] G. W.Fernando. **2008**, Chapter 4 - Magnetic Anisotropy in Transition Metal Systems. *Handbook of Metal Physics*, vol. 4, 2008, pp. 89-110
DOI: 10.1016/S1570-002X(07)00004-3

[19] J. De Clercq, A. Vansteenkiste, M. Abes, K. Temst, B. Van Waeyenberge. **2016**, Modelling exchange bias with MuMax3. *Journal of Physics D: Applied Physics,* vol.49 no. 43.
DOI: 10.1088/0022-3727/49/43/435001

[20] S. H. Yang, S. Parkin. **2017**, Novel domain wall dynamics in synthetic antiferromagnets. *Journal of Physics: Condensed Matter*, vol. 29, nu. 30.

DOI: 10.1088/1361-648X/aa752d

[21] M. P. Proenca, M. Muñoz, I. Villaverde, A. Migliorini, V. Raposo, L. Lopez-Diaz, E. Martinez, J. L. Prieto. **2019**, Deterministic and time resolved thermo-magnetic switching in a nickel nanowire. *Scientific Reports* vol. 9, Article no 17339
DOI: 10.1038/s41598-019-54043-y

[22] H. Fangohr, T. Fischbacher, M. Franchin, G. Bordignon, J. Generowicz, A. Knittel, M. Walter, M. Alber. NMAG User Manual (0.2.1), 11. Mini tutorial micromagnetic modelling
Link to the web page:
http://nmag.soton.ac.uk/nmag/0.2/manual/html/tutorial/doc.html